國 立 交 通 大 學

生物科技研究所
碩士論文

溶藻弧菌胺醯組胺酸雙胜肽酶之生化特性分析及其功能性胺基酸之研究

Characterization of Functional Residues for Catalysis and Kinetics of Aminoacylhistidine Dipeptidase from *Vibrio alginolyticus*

研究生： 陳怡親

指導教授： 吳東昆 博士

中華民國九十六年七月

Characterization of Functional Residues for Catalysis and Kinetics of Aminoacylhistidine Dipeptidase from *Vibrio alginolyticus*

研究生：陳怡親　　Student: Yi-Chin Chen

指導教授：吳東昆 博士　　Advisor: Dr. Tung-Kung Wu

國 立 交 通 大 學

生物科技研究所

碩士論文

A Thesis

Submitted to Department of Biological Science and Technology

College of Science

National Chiao Tung University

in partial Fulfillment of the Requirements

for the Degree of

Master

in

Biological Science and Technology

July, 2007

Hsinchu, Taiwan, Republic of China

中華民國九十六年七月

溶藻弧菌胺醯組胺酸雙胜肽酶之生化特性分析及其功能性胺基酸之研究

研究生：陳怡親　　指導教授：吳東昆 博士

國立交通大學 生物科技研究所碩士班

摘要

胺醯組胺酸雙胜肽酶(PepD, EC 3.4.13.3)為胜肽酶家族M20 中的一員。胜肽酶家族M20中的酵素皆屬於金屬雙胜肽酶，而經由研究發現可被應用於抗菌、癌症的臨床治療及神經傳導物質的調控等方面。過去對於細菌中胺醯組胺酸雙胜肽酶的研究很少，只針對其序列和部分生化特性進行探討，並無其生理角色或活性區胺基酸相關之研究。本論文將溶藻弧菌*pepD*基因殖入pET-28a(+)質體中，表現出N端帶有His-tag之重組蛋白，並利用Ni-NTA親和層析管柱純化之。純化出的蛋白質對於特定的Xaa-His雙胜肽(例如: L-carnosine)具有水解的能力，但無水解三胜肽之活性。經酵素動力學研究，溶藻弧菌PepD蛋白對雙胜肽L-carnosine之K_m與k_{cat}值分別為 0.36 mM與 8.6 min^{-1}。經由序列分析預測溶藻弧菌PepD蛋白上胺基酸位置His80、Asp82、Asp119、Glu149、Glu150、Asp173及His461 為活性區胺基酸。其中將所預測影響金屬鍵結之胺基酸Asp119 以及扮演催化角色之胺基酸Glu149 分別進行飽和定點突變，發現大部分之突變蛋白皆失去或降低原有之活性。此外，以同屬M20 胜肽酶家族之PepV蛋白結晶結構為模板做出溶藻弧菌PepD蛋白之同源模擬，顯示出相同之活性區胺基酸。因此，根據本論文實驗結果將首次提出胺醯組胺酸雙胜肽酶活性區胺基酸之分佈情形與其可能扮演之功能。

Characterization of Functional Residues for Catalysis and Kinetics of Aminoacylhistidine Dipeptidase from *Vibrio alginolyticus*

Student : Yi-Chin Chen Advisor : Dr. Tung-Kung Wu

Institute of Biological Science and Technology

National Chiao Tung University

Abstract

Proteins of the aminoacylase-1/metallopeptidase 20 (Acyl/M20) family were characterized to contain a zinc-binding domain at their active site. Aminoacylhistidine dipeptidase (PepD, EC 3.4.13.3) is a member of peptidase family M20 which catalyzes the cleavage and release of *N*-terminal amino acid, usually are neutral or hydrophobic residue, from Xaa-His peptide or polypeptide. We have cloned a *PepD* gene, which shared high sequence identity with PepD from various *Vibrio spp.* and 63% from *Escherichia coli* and *Salmonella typhimurium*, from *Vibrio alginolyticus*. *V. alginolyticus* PepD was expressed and purified by Ni-NTA column. The kinetics values including k_{cat} (8.6 min^{-1}), k_{cat}/K_m (0.398 $mM^{-1}s^{-1}$) of bacterial PepD were first identified. Sequence analysis revealed that Asp82 and Glu149 were probable active site residues and that Asp119, Glu150, Asp173, and His461 were probable metal ion binding residues of *V. alginolyticus* PepD. Site-directed mutations of D119 (putative metal ion binding site residue) and E149 (putative active site residue) residues of PepD exhibited activity decreasing or losing, as compared with wild-type PepD. The homology model of *V. alginolyticus* PepD, based on that of *L. delbrueckii* PepV structure, exhibited similar active site pocket as predicted. The functional role of these residues on enzyme catalysis and kinetics will be discussed in the thesis.

謝誌 (Acknowledgement)

在過去兩年的研究生活中，有苦有甘並且充滿刺激。不管在實驗上或是生活上，都接觸到許多新鮮的人、事、物。在這過程中，我對生物科技這個領域有了更深入的了解，也習得許多專業知識及實驗操作技巧，在待人接物方面也學習到很多道理。回顧這兩年，檢視自己，相信在專業領域的拓展及心靈上的成長都日益成熟。而首先要感謝的就是指導教授吳東昆 博士，給予我加入實驗室學習的機會，不僅在專業的知識背景、實驗技術及實驗設計觀念上給予指導，在生活上及待人接物方面也給予很多幫助，教導我對事情所應有的積極態度及不畏懼失敗挫折的毅力並且給予適時的鼓勵及肯定，在最後也花費了很多的心力協助論文的修改。感謝口試委員張大慈 教授與楊裕雄 教授於百忙之中抽空審閱及修改我的論文初稿，並對實驗設計觀念、操作技巧、實驗過程、結果與討論提供諸多寶貴意見，使本論文能更加完善。

感謝實驗室的大學長程翔學長，總是不斷的鼓勵我，讓我擁有更多對實驗的熱情而不會因為失敗而喪志，在最後分子模擬實驗上也給予了我很多的幫助；感謝行動百科全書裕國學長，把我從一個什麼都不會的小毛頭教導成到現在可以獨立操作實驗，不管是在實驗的設計上或是技術上的指導，都給予我相當多的幫助。並且教導我積極汲取新的知識技術的態度，感謝過去兩年來的教導和照顧；感謝庭翊學長，總是不厭其煩的替我解答大大小小的實驗問題，並且教導我學會獨立解決問題的能力，不管在實驗上或是生活事物上認真負責的態度，一直都是我努力學習的典範；感謝善解人意的媛婷學姊，在生活上對我的照顧及關心，在我低潮時給予我很大的支持及鼓勵；感謝晉豪學長，在 Circular Dichroism 和 HPLC 分析實驗上的教導和幫忙，遇到困難時總是積極的協助我找出可能的問題所在，陪我渡過只有儀器操作聲的難熬夜晚；感謝晉源學長，在我剛進入實驗室時幫助我很快的適應實驗室生活，在辛苦的純化及養晶的實驗上付出相當多的心力及幫助；感謝文鴻學長，在日常生活上的照料，並且很有耐心的替我解答一些實驗上奇奇怪怪的問題，總是在我需要幫忙時給予協助。另外感謝我最好的戰友大景，文宣和皓宇，謝謝你們不論在實驗或生活上的幫忙及照顧，總是默默的聽我抱怨並且給予我

鼓勵及支持，那些無數個一起打拼的夜晚還有講不完的蠢事都會是最好的回憶。感謝學弟妹文祥、良瑋和采婷，在我實驗期間的協助，生活上的關心及照顧，還有最後這段時間給予我的支持與鼓勵。感謝新成員禕婷、聖慈、天昶和亦諄在口試的時候細心負責的幫忙準備餐點和設備。感謝所有關心與指導過我的人，陪伴著我渡過這兩年的人，我很開心我是身為 Wu lab 的其中一員，這兩年的碩士生涯將會是我人生旅程中不可抹滅的一段精采又美麗回憶！在此分享我的成果及對所有的人致上最深的謝意和祝福。

Keywords

Vibrio alginolyticus, aminoacylhistidine dipeptidase, PepD, metallopeptidase, L-carnosine, carnosinase, peptidase M20 family

Abbreviations

APS	Ammonium persulfate
AUC	Analytical Ultracentrifugation
bp	base pair
BSA	bovine serum albumin
CD	Circular dichroism
CDC	Centers for Disease Control and Prevention
CO_2	carbon dioxide
dH_2O	distilled water
ddH_2O	double distilled water
DMF	dimethylformamide
DMSO	dimethyl sulfoxide
DNA	deoxyribonucleic acid
dNTP	deoxynucleoside triphosphate
EDTA	ethylenediamine-tetraacetic acid
ELISA	enzyme-linked immunosorbent assay
FBS	fetal bovine serum
GABA-His	γ-Amino-butyryl-histidine dipeptide
HCl	hydrogen chloride
HRP	horseradish peroxidase
H_2SO_4	sulferic acid
ICP-MS	inductively coupled plasma-mass spectrometry
IPTG	isopropyl-1-thio-β-D-galactopyranoside
kb	kilobase(s)
kDa	kiloDalton(s)

KPi	potassium phosphate
LB	Luria-Bertani
mAb	monoclonal antibody
NaCl	sodium chloride
NaN_3	sodium azide
NaOH	sodium hydroxide
NC	nitrocellulose
NCBI	National Center for Biotechnology Information
NC-IUBMB	Nomenclature Committee of the International Union of Biochemistry and Molecular Biology
NEM	*N*-ethylmaleimide
OPA	*o*-phthaldialdehyde
pAb	polyclonal antibody
PBS	phosphate buffered saline
PCR	polymerase chain reaction
PEG	polyethylene glycol
RT	room temperature
SDS-PAGE	sodium dodecyl sulfate polyacrylamide gel electrophoresis
SEM	Scanning Electron Microscopy
spp.	species
TCA	trichloroacetic acid
TEMED	*N*,*N*,*N*',*N*'-tetramethylethylenediamine
TMB	3,3',5,5'-tetramethylbenzidine
Tris base	Tris(hydroxymethyl)aminomethane
TSB	tryptic soy broth
X-gal	5-bromo-4-chloro-3-indolyl-β-D-galactopyranoside

Table of Contents

List of Figures

List of Tables

Chapter 1 Introduction

1.1 *Vibrio* species

Members of the genus *Vibrio* are defined as gram-negative bacteria possessing a straight or curved rod shape. They are motile organisms, using a single polar flagellum to travel. Most of *Vibrio spp*. are halophilic bacterial and a few species are nonhalophilic, depending on their sodium chloride requirements. *Vibrio* bacteria are commonly found in marine or estuarine environments and most species are sensitive to acid pH. They are heterotrophic organisms, obtaining nutrients from their mutualistic, parasitic, or pathogenic relationships with other organisms and can undergo both respiratory and fermentative metabolism.

In the last four decades, researches on taxonomic, environmental, virulent, and medical aspects of *Vibrio* species have expanded greatly. *Vibrio spp*. are considered as pathogens in aquacultured species. Vibriosis is a systemic bacterial infection of estuarine fishes and marine lives. On the basis of phenotypic data, the major species causing vibriosis in shrimp are *V. alginolyticus, V. anguillarum, V. harveyi*, and *V. parahaemolyticus*.[1] The *V. anguillarum*, *V. damsela*, and *V. carchariae* are major vibriosis-causing species in fish. It resulted in high mortality and severe economic loss for shrimp aquaculture in all producing countries.

Vibrio species can infect human by taking seafood or when the wound contacted with the brine. Vibriosis is caused by taking seafood contaminated with *Vibrio parahemolyticus* or *Vibrio vulnificus*. These bacteria damage the inner wall of the intestine and get into the bloodstream, which causes diarrhea and related symptoms. Another major disease caused by *Vibrio* species is cholera. Cholera is a disease of the small intestine, unlike other enteric illnesses. *V. cholerae* infect the small intestine, they get through the mucus layer and adhere to the mucosal cells where they release enterotoxins. In recent years, there is a low occurrence of *V. cholerae* by improving sewage and water treatment.

Since 1988, the Centers for Disease Control and Prevention (CDC) has maintained a database of reported *Vibrio* isolations and infections from human. There are at least twelve pathogenic *Vibrio* species recognized to cause human illness (Table 1).[2] Three species of most medical significance are *V. cholerae, V. vulnificus, and V. parahaemolyticus. V. alginolyticus, V. fluvialis, V. furnissii, V. hollisae, and V. metschnikovii*, these species are associated with gastroenteritis.[3] *V. cincinnatiensis, V. damsela*, and *V. carchariae* are not associated with gastroenteritis, but are pathogenic to human on rare occasions.

Table 1. Association of *Vibrio* spp. with different clinical syndromes.

	Clinical Syndrome[a]		
Species	**Gastroenteritis**	**Wound Infection**	**Septicemia**
V. alginolyticus	+[b]	++	
***V. cholerae* O1**	++		
***V. cholerae* non-O1**	++	+	+
V. cincinnatiensis			
V. damsela		++	
V. fluvialis	++	(+)	(+)
V. furnissii	++		
V. hollisae	++	(+)	(+)
V. metschnikovii	(+)		
V. mimicus	++	(+)	(+)
V. parahaemolyticus	++	+	(+)
V. vulnificus	+	++	++

[a] Data from Levine and Griffin,1993.
[b] ++ = common presentation, + = less common presentation, and (+) = rare presentation.

Gastroenteritis, wound infection, and septicemia are the major clinical symptoms of *Vibrio* infections. The most common clinical symptom is self-limited gastroenteritis. It often involves in stomachache, abdominal pain, diarrhea, nausea, vomiting and fever, with non-inflammatory infection of the upper small bowel, or inflammatory infections of the colon. Wounds usually occurred at the fingers, foots and palms, with rapidly progressing

swelling, hemorrhagic and severe pain after *Vibrio* infection for 3 to 24 hours. In patients with medical conditions such as cirrhosis or malignancies, the wound infection may progress very rapidly, with formation of hemorrhagic bullae and extensive soft tissue necrosis. Septicemia is a serious, life-threatening infection that gets worse very quickly and can rapidly lead to septic shock and death. It can be arised from infections throughout the body, including infections in the lungs, abdomen, and urinary tract. Patients of septicemia frequently develop fever, shaking chills, generalized myalgia, edema, and severe pain in the lower extremities. For these reasons, the infection of *Vibrio* is becoming an important public health problem to human.

1.2 *Vibrio alginolyticus*

Vibrio. alginolyticus was first recognized and named *Oceanomonas alginolytica* by Miyamoto *et al.* in 1961.[2] It was renamed *V. alginolyticus* by Sakazaki in 1968.[3] *V. alginolyticus* is one of the 12 recognised marine *Vibrio* species that have been identified as being pathogenic for humans and marine animals. It was found with worldwide distribution in marine and estuarine waters, especially in bathing areas[4] and had been isolated from coastal water, sediments, and seafood taken from the temperate and tropical areas.[5] The bacterium is able to multiply in salty waters at elevated water temperatures. It is usually isolated in the spring and summer from marine sources. However, the isolation is dependent on water temperature and it is possible to assume that *V. alginolyticus* may be isolated at any water temperatures greater than 10℃.[6] Studies by Baross and Liston showed that the minimum growth temperature for *V. alginolyticus* is 8℃.[7]

V. alginolyticus and *V. parahaemolyticus* were isolated from similar types of marine samples. In 1965, *V. alginolyticus* was designated as *V. parahaemolyticus* subgroup 2.[3] They

are very similar on biochemical properties. *V. alginolyticus* can be differentiated from *V. parahaemolyticus* on the basis of sucrose fermentation, the Voges-Proskauer reaction, sodium chloride tolerance, and swarming on blood agar (Table 2).[6]

Table 2. Differentiation of *V. parahemolyticus* and *V. alginolyticus*

Characteristic	*V. parahaemolyticus*	*V. alginolyticus*
Sucrose fermentation	−	+
Vogs-Proskauer	−	+
Growth in broth with 8% NaCl	+	+
Growth in broth with 10% NaCl	−	+
Swarming on blood agar	−	+

V.alginolyticus might infect fish with the biofilm formation on the intestine, causing fish mortalities and important economic losing.[3, 8] *V. alginolyticus* is also an important pathogen to human, first recognized as human pathogen in 1973.[9] In recent years, several studies have reported the clinical infection caused by *V. alginolyticus*.[10-12] Most human infections caused by *V. alginolyticus* were on account of consuming the raw or undercooked seafood obtained from fish, shellfish, shrimps, or squid.[13] The major clinical syndromes *V. alginolyticus* causes are gastroenteritis, wound infections, and septicemia.[14] Other clinical syndromes reported in association with *V alginolyticus* infection include ear infection, chronic diarrhea in a patient with AIDS, conjunctivitis, and post-traumatic intracranial infection.[15-17] Vibriosis caused by pathogenic *V. alginolyticus* is also a common problem in the intensive culture of grouper with a gastroenteritis syndrome (swollen intestine containing yellow fluid).[18] Therefore, *Vibrio alginolyticus* is not only an important pathogen to marine animals including fish, shellfish and echinoids but also to involve human health.

1.3 Metallopeptidase

The peptidase required metal ion for its catalytic activity was named metallopeptidase which could be divided into two board types depending on the number of the required metal ions. Metallopeptidases are the most diverse of the catalytic types of proteases with 15 clans and more than 30 families identified to date.[19, 20] In these identified families, there are seventeen endopeptidases, twelve exopeptidases and one metallopeptidases held both functions. Most of metallopeptidases require only one metal ion, but in some families they require two metal ions that act together or so called "co-catalytically". All known co-catalytic metallopeptidases are exopeptidases which include aminopeptidases, carboxypeptidases, dipeptidases, and tripeptidases, whereas metallopeptidases with only one catalytic metal ion might be exopeptidases or endopeptidases. In these enzymes, the nucleophilic attack on a peptide bond is mediated by a water molecule, which is also observed in aspartic and glutamic peptidases.[21] The water molecule was activated by a divalent metal cation, usually zinc but sometimes cobalt, manganese, nickel, or copper.

Several metallopeptidases containing co-catalytic metallo-active sites are key players in carcinogenesis, tissue repair, neurological processes, protein maturation, hormone-level regulation, cell-cycle control and protein-degradation processes.[22, 23] They are widely regarded as promising targets for drug discovery, but the detailed mechanistic information is still lack to hamper the therapeutic development. The importance of understanding their mechanism of action is underscored by their central role in several disease states including stroke, diabetes, cancer, HIV, bacterial infections, and neuropsychiatric disorders associated with the dysregulation of glutamatergic neurotransmission, such as schizophrenia, seizure disorders, and amyotrophic lateral sclerosis (ALS). For these reasons, several co-catalytic metallopeptidases have become the target for therapeutic drug designs.[24]

The majority of metallopeptidases contain two zinc ions at their active site and the residues involved in zinc binding site have been identified by X-ray crystallography. These residues usually are His, Glu, Asp, or Lys, and at least one another residue is required for catalysis, which might play an electrophilic role. With in the identified metallopeptidase familes, an HEXXH motif that form part of the metal-binding site was observed in thirteen metallopeptidases according to the crystallographic studies.[19] These zinc metallopeptidases plays roles in metabolic and signaling pathways throughout all kingdoms of life and some are regarded as potential pharmaceutical targets.[24]

1.4 Acyl/M20 Family

According to the MEROPS database (http://merops.sanger.ac.uk), each peptidase is assigned to a "family" on the basis of statistically significant similarities in amino acid sequence, whereas families that are thought to be homologous are grouped together in a "Clan". Metallopeptidases were classified into 15 clans including MA, MC, MD, ME, MF, MG, MH, MJ, MK, MM, MN, MO, MP, MQ, and M-. The peptidases in clan MH contains a variety of co-catalytic zinc-dependent peptidases that binding two zinc atoms via five amino acids per monomer, which is held by five amino acid ligands[20] and are inhibited by the general metal chelator ethylenediamine-tetraacetic acid (EDTA). In recent reports, it was considered that members of MH and MF clan of dizinc peptidases compared with MC clan of monozinc peptidases displayed three different catalytic zinc centers that have evolved in a similar structural scaffold.[25]

The peptidase clan MH is further classified into four families: M18, M20, M28, and M42. Enzymes of peptidase family M20 were characterized as water associated with two zinc ions which were bound by five residues in the order His/Asp, Asp, Glu, Glu/Asp, and His at the active site. In general, the general active site residues arrangement of metal-binding residues

with the addition of two catalytic residues (bold) would be His/Asp, **Asp**, Asp, **Glu**, Glu, Glu/Asp, His. The Asp residue between two catalytic residues was considered to bind both metal ions. The essential histidine and carboxyl residues in the metal binding sites of all enzymes of this family, were found to be completely conserved.

Peptidase family M20 could be further devided into 4 subfamilies, M20A, M20B, M20C, and M20D, which their active site residues were different among subfamilies. The type protein of peptidase family M20C is aminoacylhistidine dipeptidase which could hydrolyze Xaa-His dipeptides. Several available crystal structures of M20 family enzymes, including PepV, CPG2, showed a dizinc-binding domain. Enzymes of the Acyl/M20 family have shown potential for different applications. In biocatalysis, the high stereoselectivity of Acy1 allows the preparation of L-amino acids from racemic mixtures of *N*-acyl-L-amino acids.[26] Succinyldiaminopimelate desuccinylase is considered as a potential anti-bacterial target, and CPG2 is considered as a therapeutic agent in ADEPT for cancer treatment.[27]

1.5 Aminoacylhistidine Dipeptidase

The *pepD* gene exists extensively among the prokaryotes and eukaryotes. Some studies have suggested that expression of *pepD* negatively affected biofilm formation which was considered for infection, causing fish mortalities and important economic loss. Therefore, PepD could be a promising target to control bacterial biofilm formation and infection.[28] In *E. coli, pepD* encodes a 52 kDa protein and is active as a homodimer with molecular mass of 100 kDa. The board substrate specificity of PepD was activated by Co^{2+} and Zn^{2+} and deactivated by metal chelators.[29, 30] The first direct proof of aminoacylhistidine dipeptidase (EC 3.4.13.3, also Xaa-His dipeptidase, X-His dipeptidase, carnosinase, and PepD) activity for hydrolysis of an unusual dipeptide L-carnosine (β-Ala-L-His) in bacteria was obtained with *Pseudomonas aeruginosa* in 1974.[31] In the following years, this carnosine-hydrolyzing

enzyme is discovered from a number of bacterial species,[32] but only PepD from *Escherichia coli* have been characterized genetically and biochemically.[30] Aminoacyl-histidine dipeptidases are zinc-containing metallopeptidase, whose catalytic reaction involved the release of an N-terminal amino acid, usually neutral or hydrophobic, from a polypeptide. PepD could hydrolyze Xaa-His dipeptides even include an unusual dipeptide carnosine (β-Ala-L-His) toβ-Alanine and L-Histidine(Fig. 1).[19]

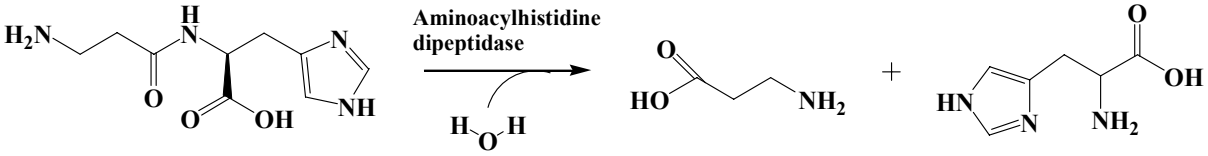

Fig. 1 Reaction result in liberated L-histidine from L-carnosine hydrolyzation.

In general, dipeptidases are involved in the final breakdown of protein degration fragments produced by other peptidases or the final dipeptide breakdown for amino acid utilization. The same result was observed in PepD-deficient mutant of *E. coli*[33] and *S. typhimurium*[34], which indicates that PepD hydrolyzes dipeptide for the amino acid source. However, the biological impact of PepD still remains unclear.

1.6 Carnosine

The enzymes with L-carnosine hydrolyzing activity were also observed in mammals and named as carnosinase in general. The unique substrate of carnosinase, L-carnosine (β-alanyl-L-histidine), was first isolated in 1990 from meat extracts and subsequently found to be widely distributed in excitable central and peripheral vertebrate tissues. It is abundant in skeletal muscles of most vertebrates and constantly present in cardiac muscle and brain in millimolar concentrations (1.7–2.5 mM in whole brain,0.15–0.25 mM in medulla oblongata and ≥ 10 mM in olfactory bulb), but not in several other organs, such as kidney, liver, and

lung.[35] The concentration of this dipeptide is regulated by two enzymes, carnosine synthase and carnosinase, both of which are present in brain.

The complete role of these dipeptides is still unknown, even though their function has been studied intensively in recent years. Available studies indicated that carnosine has a range of antioxidant or cytoprotective properties,[36] to act as a cytosolic buffer,[37] an antioxidant,[38] and an antiglycation agent.[39] The unique dipeptide has been proposed that could act as a natural scavenger of dangerous reactive aldehydes from the degradative oxidative pathway of endogenous molecules such as sugars, polyunsaturated fatty acids (PUFAs) and proteins. In particular, it has been recently demonstrated that carnosine is a potent and selective scavenger of α,β-unsaturated aldehydes, typical by-products of membrane lipids peroxidation and considered second messengers of the oxidative stress, and inhibits aldehyde-induced protein-protein and DNA-protein cross-linking in neurodegenerative disorders such as Alzheimer's disease, in cardiovascular ischemic damage, in inflammatory diseases.[40]

Moreover, carnosine represents the archetype of a series of histidine-containing dipeptides in mammals, such as homocarnosine (γ-aminobutyric acid-L-histidine), carcinine, *N*-acetylcarnosine, and anserine (Fig. 2). Homocarnosine was suggested to be a precursor for the neurotransmitter GABA. Being controlled by one or several carnosinases, it acts as a GABA reservoir and may mediate the antiseizure effects of GABAergic therapies.[41]

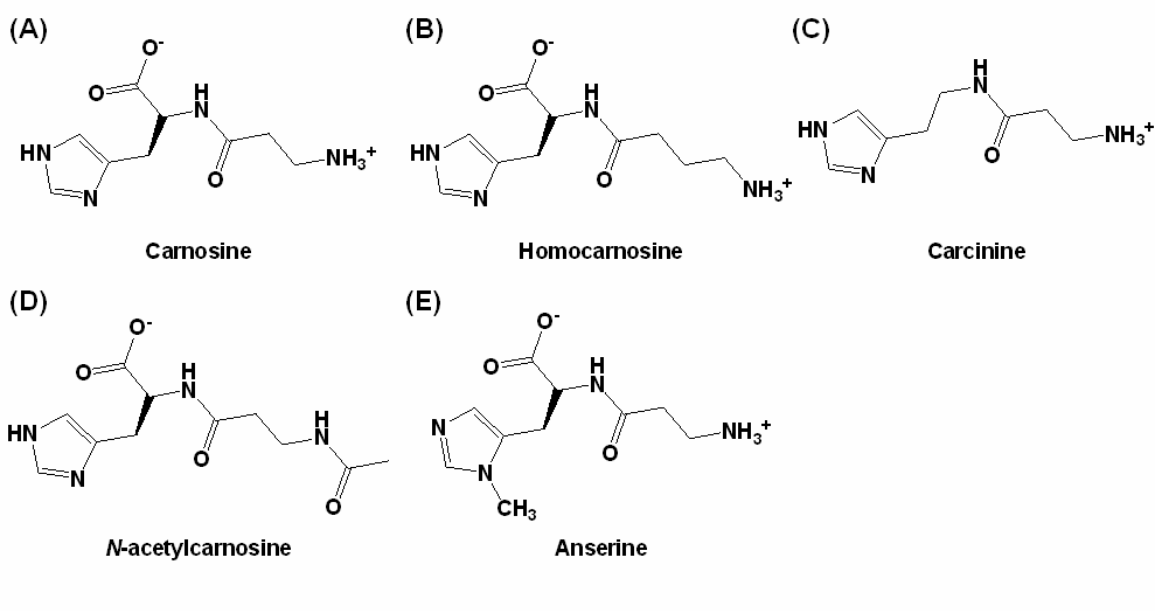

Fig. 2 Common histidine-containing dipeptides present in mammals.

1.7 Carnosinase

Carnosine is synthesized by carnosine synthase (EC 6.3.2.11) from β-alanine and histidine in many tissues and degraded by intra- or extracellular dipeptidases, also named carnosinases, all belonging to the large family of metalloproteases. In mammals, at least two types of carnosinases with different properties. The first enzyme is serum carnosinase (CN1, EC 3.4.13.20)[42] and the second one is known as a cytosolic form (also named tissue carnosinase, CN2, EC 3.4.13.18). Serum carnosinase (CN1) was identified as a homodimeric dipeptidase with a narrow substrate specificity for Xaa-His dipeptides including L-carnosine. The nature of metal ion in serum carnosinase remains unknown and could be activiated by Cd^{2+} and citrate ions.[43] It could also hydrolyze homocarnosine and anserine, and these activities were not inhibited by bestatin, a compound known to specifically inhibit various amino- and dipeptidases.

Serum carnosinase was assumed to be involved in some important pathological conditions. Decreased concentrations of serum carnosinase have been observed in patients

with Parkinson's disease, multiple sclerosis, or after a cerebrovascular accident.[44] It was also suggested that monitoring of serum carnosinase might be useful to predict the clinical symptom of patients with acute stroke.[45] Deficiency of human carnosinase has been associated with neurological deficits including intermittent seizures and mental retardation.[46, 47] Study on serum carnosinase was also approached by computational analysis that suggested a therapeutic usefulness of either inhibiting by L-carnosine analogues (e.g., in diabetes) or activating the enzyme by the rational design of citrate-like, non-toxic allosteric modulators (e.g., in homocarnosinosis).[48]

Tissue carnosinase (CN2) was first isolated from porcine kidney by Hanson and Smith in 1949[49] and subsequently found widely distributed in tissues of rodents and higher mammals. It acted as an ubiquitous nonspecific dipeptidase rather than a selective carnosinase with broad substrate specificity but could not hydrolyze homocarnosine or anserin.[42] This enzyme requires Mn^{2+} ions for its activity and is strongly inhibited by low concentrations of bestatin.

1.8 Other Carnosine-Hydrolyzing Enzymes

There are also some other proteins reported to have the dipeptidase activity on L-carnosine. BapA from *Pseudomonas* sp. proposed as β-Ala-Xaa dipeptidase (EC 3.4.13.-) was found to hydrolyze peptide bonds of β-alanyl dipeptides (β-Ala-Xaa).[50] Pep581 from *Prevotella* species (*Prevotella* spp.) shared similar sequence identity of 47% with *E. coli* PepD and has a calculated molecular weight of 53.2 kDa. Pep581 hydrolyzed both dipeptides and single amino acid from the *N*-terminus of tri- and oligopeptides, which is different from PepD enzymes.[51] Anserinase (Xaa-methyl-His dipeptidase, EC 3.4.13.5) mainly catalyzing the hydrolysis of *N*-acetylhistidine in all poikilothermic vertebrates is also active on carnosine.

1.9 Peptidase V

Lactobacillus delbrueckii pepV is 1413 nucleotides in length and consists of 470 amino acid residues, encodes a protein with predicted molecular mass of 52 kDa. *Lactobacilli* are organisms with multiple amino acid auxotrophies making them critically dependent on their proteolytic abilities to efficiently degrade milk protein casein and used as starting materials in their dairy fermentations. Deletion of the dipeptidase *pepV* gene from *Lactobacilli* resulted in significantly decreased growth rates but did not reduce the final cell density.[52]

The Peptidase V (PepV) from *Lactobacillus delbrueckii* ssp. *lactis* DSM 7290 was originally identified as a carnosinase, cleaving L-carnosine as a source of histidine, in the *E. coli* mutant strain UK197 (*pepD*, *hisG*).[53] It has also been characterized as a relatively unspecific dipeptidase cleaving a variety of dipeptides, especially those with the unusual β-alanyl residue in the *N*-terminus, and removing the *N*-terminal amino acid from a few distinct tripeptides.[53] Moreoner, PepV is related not only to peptidases but also to acetylornithine deacetylase (ArgE, EC 3.5.1.16) and succinyldiaminopimelate desuccinylase (DapE, EC 3.5.1.16), and has been described as a member of the aminoacylase-1 family recently.[54] These enzymes share the characteristics of hydrolyzing amide bonds in a zinc- (or cobalt-) dependent manner. Therefore, PepV is recognized as a metallopeptidase in M20A subfamily from MH clan. It could be fully inhibited with metal chelating agent 1, 10-phenanthroline or EDTA.

PepV is the first crystallized dinuclear dipeptidase with carnosine-hydrolyzing enzymatic activity in M20 family. The 3D structure of PepV protein consists of two distinc domains, named the lid (lower) domain and the catalytic (upper) domain. The upper domain contains the polypeptides from Met1 to Gly185 and from Ser388 to Glu468, whereas the lid domain comprises the residues from Glu186 to Gly387. In the crystal structure of PepV, two zinc

ions is associated in one monomer protein.[55] Zinc ions are located in the catalytic domain and held by five residues including His87, Asp119, Glu154, Asp177, and His439 (Fig. 3).[55]

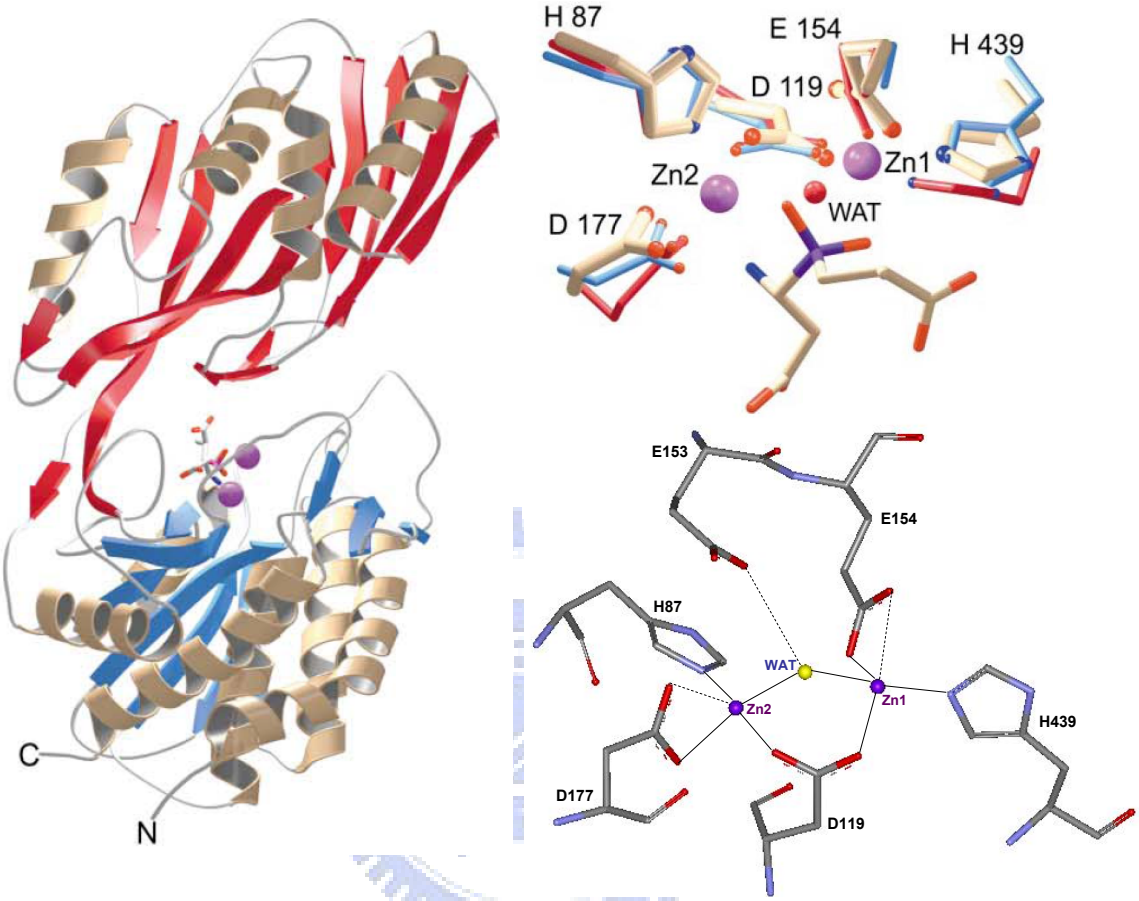

Fig. 3 The Overall structure of PepV and the stereo view of catalytic and zinc binding residues of PepV. The inhibitor of PepV (beige) superimposed with the zinc binding residues of AAP (blue) and CPG2 (red). Residues are numbered according to the PepV sequence. The catalytic water molecule of CPG2 is depicted in red (WAT).

These two zinc ions, as described by *Jozic et al.*,[55] were considered to play two different roles for hydrolyzing substrates: for stabilization of the substrate-enzyme tetrahedral intermediate as well as for activation of the catalytic water molecule (Fig. 4). Zinc 1 which associated with the imidazole group of H439, carboxylate oxygen of E154 and D119 primarily appeared to facilitate substrate binding via a "oxyanion binding hole" with H269

resulting in polarize the scissile carbonyl group and therefore to promote the nucleophilic attack by the catalytic water molecule. Zinc 2 was coordinated by the carboxylate oxygen of H87, D177 and the bridging D119. It seemed primarily to activate the catalytic water molecule and to promote binding and hydrolysis.

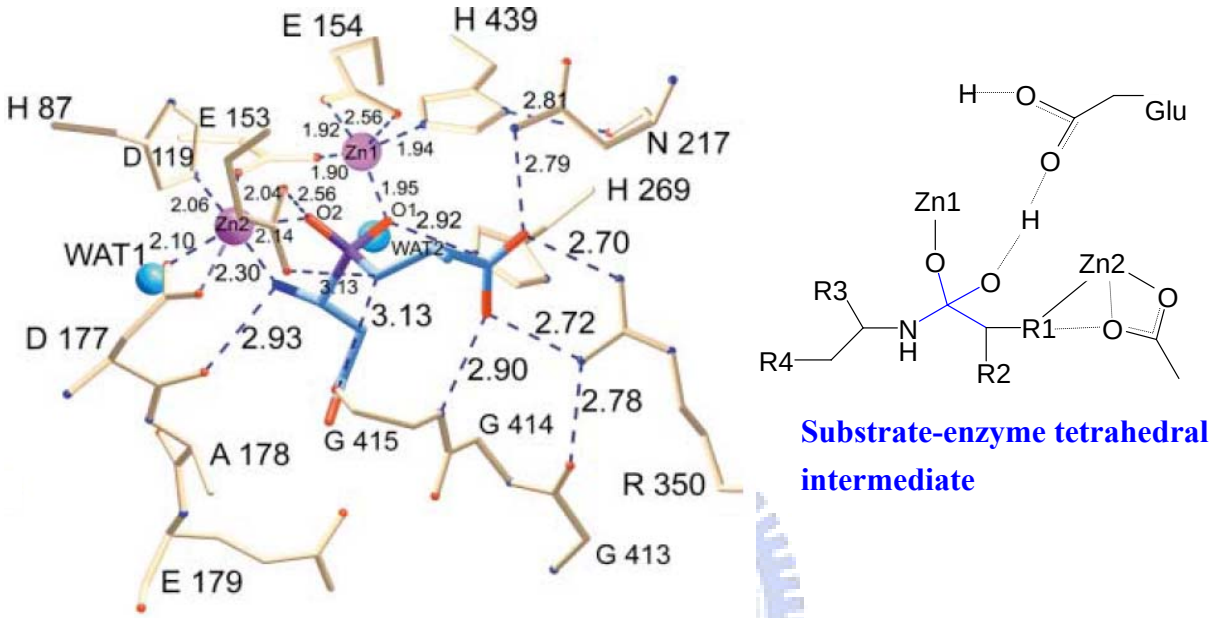

Substrate-enzyme tetrahedral intermediate

Fig. 4 Schematic of the active site of PepV. The Asp-Ala phosphinate inhibitor mimics the dipeptide substrate is shown in blue. The bridging catalytic water attacks the carbonyl carbon of the scissile peptide bond to form a sp^3-orbital substrate-enzyme tetrahedral intermediate.

The PepV catalytic domain has similar folding relative to that previously found dinuclear carboxyl exo-peptidases AAP,[56] SGPA[57] and CPG2.[58] There is a *cis*-peptide bond between the bridging Asp119 and the adjacent residue Asp120 in PepV which was also observed in these enzymes. In both di-zinc and mono-zinc carboxypeptidases of M20 family, this *cis*-conformation generally occurred in those regions of a structure intimately associated with catalysis and seems to be necessary to force the important zinc bridging carboxylate into the correct geometry.

1.10 Research Goal

V. alginolyticus, an important pathogen to human and fish, might infect fish with the biofilm formation on the intestine. Some studies have suggested that expression of *pepD* negatively affects biofilm formation, it could be a promising target to control bacterial biofilm formation and infection. Aminoacyl-histidine dipeptidases (pepD) which exists extensively among prokaryotes and eukaryotes belong to metallopeptidase 20 (M20) family from metallopeptidase H (MH) clan (MEROPS: The peptidase database). It could hydrolyzes Xaa-His dipeptides including an unusual dipeptide carnosine (β-Ala-L-His), which is benefited to organisms at several physiological aspects. Both the biological importance and function of aminoacylhistidine dipeptidase and L-carnosine are less known. Enzymes of peptidase M20 family have showed the potential for different applications which can act as anti-bacterial target, therapeutic agent for cancer treatment and possibly play roles in aging and neurodegenerative or psychiatric. Since the latent importance of bacterial aminoacylhistidine dipeptidase in biological aspect, additional with the studies on it is indispensable either in the genetic or biochemical aspect from *E. coli* and *S. typhimurium*. We perform a study on aminoacylhistidine dipeptidase from *V. alginolyticus* through gene expression, protein purification and biochemical properties characterization. Due to neither investigations on its functional residues nor crystal structure are reported, a study of the functional residues of *V. alginolyticus* PepD through site-directed mutagenesis analysis are performed.

Chapter 2 Methods

2.1 Expression of *Vibrio alginolyticus pepD* gene in *E. coli*

We used pET-28a(+) as the expression vector. The constructed plasmid pET-28a(+)-pepD was transformed into *E. coli* BL21(DE3)pLysS competent cell by heatshock method and spread the cell on LB_{kan} agarose plate and incubated at 37 ºC for 12 to 16 hrs. Picked up the clonies harboring pET-28a(+)-pepD and cultured in 3 ml LB_{kan} medium for several hours then transferred into 300 mL LB_{kan} medium. Added 150 μL 1 M IPTG (final concentration was 0.5 mM) when the OD_{600} approach 0.5 ~ 0.6, then incubated at 37 ºC for another 6 hrs for induction of the expression of pepD. The pET-28a(+) plasmid was also transformed into *E. coli* BL21(DE3)pLysS competent cell and following the same experimental procedure as a control.

2.2 Purification of expressed *Vibrio alginolyticus* PepD

After 6 hrs incubation at 37 ºC with rotary shaking, the cell was collected by centrifugation at 6,500rpm for 30 min at 4 ºC. The bacterial pallet was resuspended with 20 ml 20 mM Tris-HCl, 0.5 M NaCl, pH 6.8 buffer (buffer A). The resuspended cells were disrupted by sonication method using a sonicator with pulsing on 2 sec and pulsing off 1 sec for the toatal sonication time of 3 min at 30% energy. The whole experimental procedure of sonication was operated on ice. Repeat the sonication steps at least 3 times. After sonication, the cell lysate was centrifuged at 9,500rpm for 30 min at 4 ºC to remove the cell debris and intact cell. The supernatant was collected for further purification.

The supernatant was purified by affinity chromatography with Ni-NTA column. One mL Ni-NTA resin was packed in 20 mL plastic column and pre-equilibrated with 10 mL buffer A containing 20 mM imidazole (10 bed volumn). The supernatant was load into the column then washed with 10 ml buffer A contained 20 mM imidazole (5 bed volumes). Five bed

volumes of buffer A contained 80 mM, 150 mM, 300 mM, and 500 mM imidazole were used sequentially to elute the expressed pepD protein. At last, washing the Ni-NTA column with buffer A containing 1 M imidazole. The eluted fractions were collected for SDS-PAGE analysis and enzymatic activity assay. By SDS-PAGE analysis, the high purity eluted fractions were collected and dialyzed with 2 L 50 mM Tris-HCl pH 6.8 buffer for 2 hrs and following 3 L for 8 hrs. After enzymatic activity analysis, the purified proteins were stored at -80 ºC before ready for following experiments. PepD could be stored at -80 ºC without losing of activity for six months.

2.3 Protein concentration determination

The protein concentrations of purified proteins were measured by BCA Protein Assay Reagents. Each well of the F96 MicroWell™ plate were added 20 μL sample and mixed with 200 μL BCA™ Working Reagents (BCA™ Reagent A:BCA™ Reagent B = 50:1). The reaction were incubated at 37 ºC for 30 min in dark. The absorbances of samples were measured at 562 nm on Multiskan Ascent Microplate Reader. A 2 mg/mL bovine serum albumin (BSA) stock and successive dilutions (1.5, 1.0, 0.75, 0.5, 0.25, 0.125, 0.025 mg/mL) followed in the same procedure as described above were served as standards.

2.4 SDS-PAGE and Native-PAGE analysis

After expression and purification, gel electrophoresis was used to check the expression level, protein purity, and determination of the molecular weight. The samples were electrophoresed on a 12.5% sodium dodecyl sulfate polyacrylamide gel electrophoresis (SDS-PAGE) (Table 3). Each 10 μL sample was mixed with 2 μL 5X SDS-PAGE sample buffer and incubated at 95 ºC for 5 min to denature proteins. The electrophoresis was performed with 1X SDS-PAGE running buffer at 90 Volt for 30 min following 120 Volt for 1.5 hrs. The SDS-PAGE was stained with stain buffer containing Coomassie Brilliant blue

R-250 for 30 min and destained with destain buffer I (methanol/acetic acid/water = 4:1:5, v/v/v) for 20 min and following destain buffer II (methanol/acetic acid/water = 1.2:0.05:8.75) overnight.

Native-PAGE was performed to check the native form of PepD. The purified and dialyzed proteins fractions were electrophoresed on a 7.5% Native-PAGE (Table. 3). The experimental steps were similar to SDS-PAGE analysis besides the gel containing no SDS and without denaturing treatment. Each 10 μL sample was mixed with 2 μL 5X Native-PAGE sample buffer and was performed immediately with iced 1X Native-PAGE running buffer at 90 Volt for 3 hrs with 4 ºC circulating water bath. The proteins were stained and destained in the same way as SDS-PAGE analysis.

Table 3. Solutions and volumes for preparation of SDS-PAGE and Native-PAGE separating gel and stacking gel.

	Separating gel						Stacking gel
	7.5%	10%	12%	12.5%	15%	20%	4%
ddH_2O (mL)	16.8	13.88	11.55	11	8.05	2.22	1.7
1.5 M Tris-HCl, pH 8.8 (mL)	8.75	8.75	8.75	8.75	8.75	8.75	-
1 M Tris-HCl, pH 6.8 (mL)	-	-	-	-	-	-	1.25
10 % SDS (mL)[a]	0.35	0.35	0.35	0.35	0.35	0.35	0.1
30% acrylamide / 1% *N,N'*-methylenediacrylamide (mL)	8.75	11.67	14	14.6	17.5	23.33	0.01
TEMED (mL)	0.028	0.014	0.014	0.014	0.014	0.014	6.8
10 % Ammonium persulfate (APS)[b] (mL)	0.35	0.35	0.35	0.35	0.35	0.35	10
Total (mL)	35	35	35	35	35	35	10

[a] Replace SDS with ddH_2O when preparing Native-PAGE

[b] Recommended to prepare freshly and mix at last

2.5 Western blotting analysis

After gel electrophoresis, the resultant Native-PAGE and a nitrocellulose (NC) membrane were soaked instantly in the transfer buffer. Following transferred the protein immediately to an NC membrane with a blotting apparatus at 90 Volt for 1 hr, the NC membrane was blocked with blocking buffer for 1 hr at RT. The membrane was then washed 3 times with 1X PBS buffer and incubated with the primary anti-PepD monoclonal antibody (mAb) at 1:1,000 dilutions with 1X PBS buffer for 1 hr at RT with gentle shaking, followed by washed 5 times with 1X PBST buffer to remove the unbound primary antibodies. The washed membrane was further incubated with the goat anti-mouse IgG conjugated HRP at 1:5,000 dilutions with 1X PBS buffer for 1 hr at RT with gentle shaking. Finally, the membrane was washed with 1X PBST buffer for 5 times. The immunoreactive bands were visualized with a chemiluminescence reagent and the autoradiography film.

2.6 Enzymatic activity assay of *Vibrio alginolyticus* PepD

The PepD activity was determined according to Teufel *et al.*[42] on the basis of measurement of histidine by using of the *o*-phthalaldehyde (OPA) reagent. The substrate L-carnosine (β-Ala-L-His) would be hydrolyzed to β-Alanine and L-Histidine. The fluorescence of the derivative of histidine with OPA was detected at λ_{Ex}: 355 nm and λ_{Em}: 460 nm.

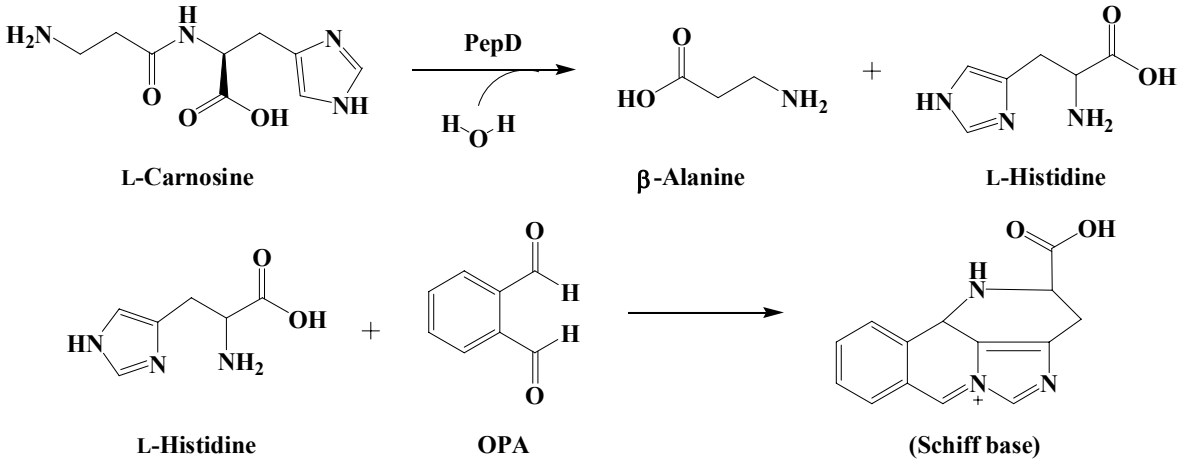

There were 20 μL purified enzyme (0.5 mg/mL) and 80 μL 50 mM Tris-HCl pH 6.8 buffer reacted with 0.5 mM L-carnosine for 20 min. Liberated histidine was derivatived by adding 100 μL OPA reagent and incubated at 37 ºC in darkness for 5 min. The reaction containing only buffer with L-histidine and L-carnosine reacted with OPA were served as positive and negative control, respectively. All reactions were carried out in triplicate. Fluorescence of the histidine derivatived with OPA was measured by Fluoroskan Ascent FL. (λ_{Ex}: 355 nm and λ_{Em}: 460 nm).

2.7 Substrate specificty of *Vibrio alginolyticus* PepD

To investigate the substrate specificity of PepD, various Xaa-His dipeptides, including β-Ala-L-His (L-carnosine), α-Ala-L-His, Gly-His, Val-His, Leu-His, Ile-His, Tyr-His, Ser-His, His-His, β-Asp-L-His, and γ-Amino-butyryl-His (GABA-His, homocarnosine) and two histidine-containing tripeptides, Gly-Gly-His and Gly-His-Gly, were used. The activity on L-carnosine was defined as 100%. The enzymatic activity analysis method and reaction condition were as described on 2.6.

2.8 Enzyme Kinetics

For determination of V_{max}, K_m, and k_{cat} of *V. alginolyticus* PepD and compared the hydrolysis efficiency with the wild-type and mutant PepD, the method described by Csámpai *et al.*[59] was modified to use by using High Performance Liquid Chromatography (HPLC) with Fluorescence Detector (FLD). The system, which consists of Agilent 1100 Series Quaternary pump, Autosampler, Fluorescence Detector and Inertsil ODS-3 (7 μm, 7.6 mm×250 mm) column, was used. The eluent system consisted of two components: eluent A was 0.05 M sodium acetate of pH 7.2, while eluent B was prepared from 0.1 M sodium acetate–acetonitrile–methanol (46:44:10, v/v/v) (titrated with glacial acetic acid or 1 M sodium hydroxide to pH 7.2). The gradient program was as described on Table 4. The fluent

flow-rate was 0.8 mL/min at 30 ºC.

Table 4. The fluent gradient program

Step	Time (min)	A (%)	B (%)
1	0	100	0
2	5	50	50
3	15	0	100
4	25	0	100

Different concentrations of L-carnosine (1, 0.5, 0.25, 0.1, 0.05, 0.025, 0.01, 0.005, and 0.0025 mM) were added as substrates to initiate enzymatic reactions. After 20 min incubation at 37 ºC, the samples were mixed with OPA reagent for 5 min incubation at 37 ºC then injected by autosampler. Fluorescence of the histidine with derivatived OPA was measured by FLD (λ_{Exc}: 355 nm and λ_{Em}: 460 nm). Various concentration of L-histidine solution (0.05, 0.025, 0.01, 0.005, 0.0025, 0.001, 0.0005, 0.00025, and 0.0001 mM) derivatived with OPA reagent were detected as method described above to serve as standards.

2.9 Site-directed mutagenesis on *Vibrio alginolyticus pepD*

Site-directed mutagenesis was performed by using the QuickChange site-directed mutagenesis kit to create the mutants. Mutagenic primers were designed and pET-28a(+)-pepD plasmid (wild-type) was used as the template: the PCR reaction was carried out by using the nonstrand-displacing action of *pfuTurbo* DNA polymerase to extend and incorporate the mutagenic primers (Appendix 1.), and resulting in the nicked circular strands. The PCR mutagenesis reaction was performed in the 96-well GeneAmp® PCR System 9700 Thermal Cycler as recommended by the manufacturer of *PfuUltra*™ High-Fidelity DNA polymerase. Each reaction added 100 ng of wild-type plasmid, 5 μL 10X *Pfu* polymerase buffer, 4 μL 2.5 mM dNTP mix, 1 μL of each 12.5 μM primer, 1 μL (2.5 U) *Pfu* polymerase and ddH_2O to the final volume of 50 μL (Table 5). The PCR products with

wild-type and mutant plasmids were incubated with *Dpn*I for 4 hrs at 37 ºC to selectively digest the methylated, non-mutated parental wild-type plasmids. After *Dpn* I digestion, the mutant plasmid was transformed into *E. coli.* XL1-Blue competent cells, with selection for kanamycin resistance. After the successful mutagenesis confirmed by restriction enzymes and DNA sequencing of plasmid, the desired mutant plasmids were transformed into *E. coli* BL21(DE3) pLysS competent cells for expression of the mutant pepD proteins.

Table 5. Reaction conditions and cycling parameters for the PCR mutagenesis reaction

pET-28a(+)-pepD plasmid	0.5
Pfu polymerase (2.5U/μL)	1
10X *Pfu* polymerase buffer	5
Primer 1 (12.5 μM)	1
Primer 2 (12.5 μM)	1
dNTP mix (2.5 mM each)	4
ddH_2O	37.5
Total	50 μL

Segment	Cycles	Temperature	Time
1	1	95 ºC	2 minutes
2	18	95 ºC	30 seconds
		52 ºC	1 minute
		72 ºC	8 minutes
3	1	72 ºC	10 minutes
4	1	4 ºC	pause

2.10 Circular dichroism (CD) spectroscopy

The secondary structure of the wild-type and the mutant pepD proteins were confirmed by monitoring CD spectra. The protein sample concentration was 0.2 mg/mL in 50 mM Tris-HCl, pH 6.8 buffer. The CD spectra were recorded every 1 nm between 200 to 300 nm wavelength used a quartz cuvette of 1 mm path-length in a Jasco J-715 spectropolarimeter, Only 50 mM Tris-HCl, pH 6.8 buffer was as the control. The results were scanned 4 times and averaged. Converted the data into mean residue ellipticity (MRE) by using the equation : $〔\theta〕_{MRE} = (MRW \times \theta_{obs}/c \times d)$.[60] θ_{obs} is the observed ellipticity (in millidegrees) at the respective wavelength, MRW is the mean residue of the enzyme ($MRW = M/n$, M = 53548.8 g/mole, n = 490 amino acid residues), d is the cuvette path-length in cm, and c is the protein concentration in mg/mL.[60]

2.11 Crystallization

Purified recombinant PepD was produced as previously described on 2.2. The purified enzyme was concentrated to 10 mg/mL and dialysed to against Tris-HCl buffer with 20 mM HEPES buffer by Centricon YM30. Using the hanging drop technique, one small droplet of the sample mixed with crystallization reagent was dropped on a siliconized glass cover slide, and the cover slide would invert to over the reservoir in vapor equilibration with the reagent. In this experiment, hanging drops were formed by mixing 1 μL enzyme solution with 1 μL of crystallization reagent at 20 ºC with the reservoir solution.

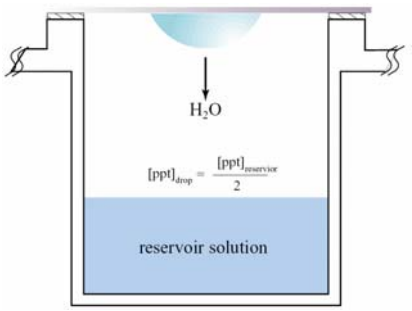

2.12 Analytical Sedimentation Velocity Ultracentrifugation

Sedimentation velocity is an analytical ultracentrifugation (AUC) method that measures the molecular moved rate for providing both the molecular mass and the shape of molecules.[61] This technique can distinguish the native state of the protein in either a monomer, dimmer, or even tetramer form. The data were evaluated according to the g*(s) method developed by Walter Stafford.[62] Since the g*(s) analysis yields both the sedimentation coefficient *s* from the peak of the curve, the apparent molecular weight can also be determined. Depending on the application and optical system, the protein concentration ranging 0.1 mg/mL to 0.5 mg/mL was used and the sample volume was about 500 μL. Sample was equilibrated with 20 mM Tris-HCl pH 6.8 buffer and this equilibrated buffer was used as another reference control into the reference sector. The sedimentation velocity analysis was performed at National Tsing Hua University.

Chapter 3 Results

3.1 Expression and Purification of *Vibrio alginolyticus* PepD

Vibrio alginolyticus PepD was sucessfully expressed in *E. coli* BL21(DE3)pLysS and purified by Ni-NTA column chromatography. The Ni-NTA resin-bound PepD would be eluted with high purity by 20 mM Tris-HCl, 0.5 M NaCl, pH 6.8 buffer containing 150 mM imidazole. The pure elutent fraction was collected and dialyzed with 20 mM Tris-HCl, pH 6.8 buffer at 4 ºC to remove the salts. The dialyzed protein on SDS-PAGE revealed a single band with molecular mass of approximately 55 kDa (Fig. 5), quite close to the calculated molecular mass, 53.6 kDa, of *Vibrio alginolyticus* PepD. The purified *Vibrio alginolyticus* PepD was also confirmed by Western blotting with an anti-PepD mAb (Fig. 5).

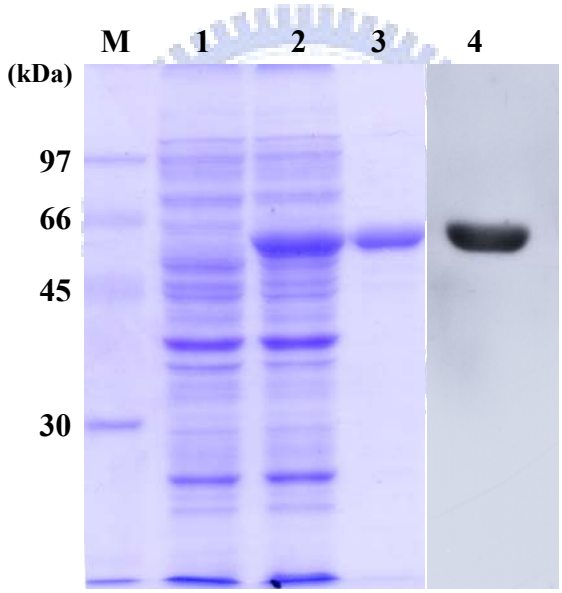

Fig. 5 SDS-PAGE and Western blot analysis of purified PepD
(a) Lane M:LMW protein marker;Lane 1:cell crude extracts of *E.coli* BL21(DE3)pLysS carrying pET-28a(+); Lane 2:cell crude extracts of *E.coli* BL21(DE3)pLysS carrying pET-28a(+)-pepD; Lane 3:purified PepD from Ni-NTA column; Lane 4:western blotting analysis of purified PepD with anti-PepD mAbs

The concentration of purified PepD was determined by BCA Protein Assay Reagent and in total 5 mg pure PepD from 300 mL *E. coli* cells could be abtained. The purified PepD was further characterized with the activity assay as described in 2.6.

3.2 Enzymatic activity assay

As described in 2.6, the purified wild-type PepD was subjected to the activity assay with L-carnosine as a substrate, which would be hydrolyzed to β-alanine and L- histidine. According to Teufel *et al.*[42] on the basis of measurement of histidine by use of *o*-phthalaldehyde (OPA) reagent. The histidine-OPA derivative was detected at λ_{Ex}: 355nm and λ_{Em}: 460nm. The purified PepD was confirmed as a member of carnosine-hydrolyzing enzymes capable of catalyzing the hydrolysis of L-carnosine to β-alanine and L-histidine which further producing the detectable fluorescence derivative of L-histidine while reacting with OPA reagent in 50 mM Tris-HCl, pH 6.8 buffer.

3.3 Substrate Specificity of *Vibrio alginolyticus* PepD

The PepD from *E. coli* has been identified as a dipeptidase with broad substrate specificity.[30] The substrate specificity of PepD from *Vibrio alginolyticus* was determined with eleven Xaa-His dipeptides, two non Xaa-His dipeptides, and two His-containing tripepides, and compared with the data from *E. coli*. The experimental method was as described in 2.7. The enzyme activity on L-carnosine (β-Ala-L-His), the known substrate of aminoacylhistidine dipeptidase (PepD), was defined as 100% (Fig. 6). The highest enzyme activity was observed from the hydrolysis of His-His, which was about two times higher than that of the L-carnosine. Moreover, the hydrolysis of α-Ala-L-His, which only differs in the orientation of the alanine also showed 1.5 times higher activity than L-carnosine hydrolysis. The relative dipeptidase activities with the other Xaa-His dipeptides substrates including Val-His, Leu-His, Tyr-His, Ile-His and Ser-His were also superior to that of carnosine degradation, and the enzyme could also hydrolyze Gly-His with good activity. The enzyme showed no apparent activity toward β-Asp-L-His and γ-Amino-butyryl-His (GABA-His, homocarnosine). In addition, the non-Xaa-His dipeptides including His-Ile, His-Val, as well as tripeptides containing histidine in the central or C-terminal position were not degraded,

indicating that *V. alginolyticus* PepD is a dipeptidase in activity.

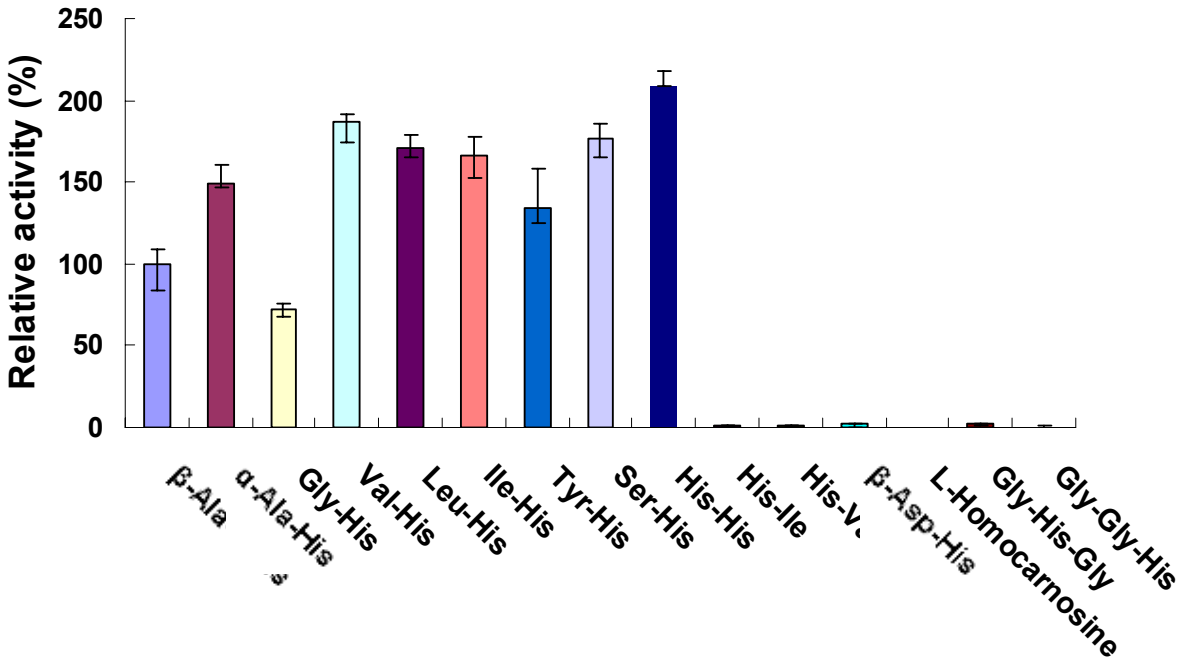

Fig. 6 Substrate specificity of PepD for Xaa-His dipeptides and histidine-containing tripeptides. Purified recombinant PepD proteins were incubated for 25 min at 37 ºC with 11 Xaa-His dipeptides, 2 non Xaa-His dipeptides and 2 His-containing tripepides, and the activity was measured as standard activity assay (see 2.6). Values are expressed as relative activity setting the degradation of carnosine to 100%

3.4 Enzyme Kinetics of *Vibrio alginolyticus* PepD

The enzyme kinetics of *V. alginolyticus* PepD for L-carnosine was performed as described in 2.8. The V_{max} and K_m values of *V. alginolyticus* PepD (2 μg, 0.186 μM) for L-carnosine calculated from the respective Lineweaver-Burk plot were 1.6 μM/min and 0.36 mM, respectively (Fig. 7). Therefore, the turnover number (k_{cat}, $k_{cat} = V_{max}/[E]_T$) of *V. alginolyticus* PepD for L-carnosine in 50 mM Tris-HCl, pH 6.8 at 37 ºC was 8.6 min^{-1} and the catalytic efficiency (k_{cat}/K_m) was 0.398 $mM^{-1}s^{-1}$. The determined K_m value of PepD was 5.64 mM from *E. coli*[30] and 0.25 mM from *S. typhimurium*[34]. The other kinetics values including

k_{cat}, k_{cat}/K_m, and specific activity of PepD, however, were first identified.

(a)

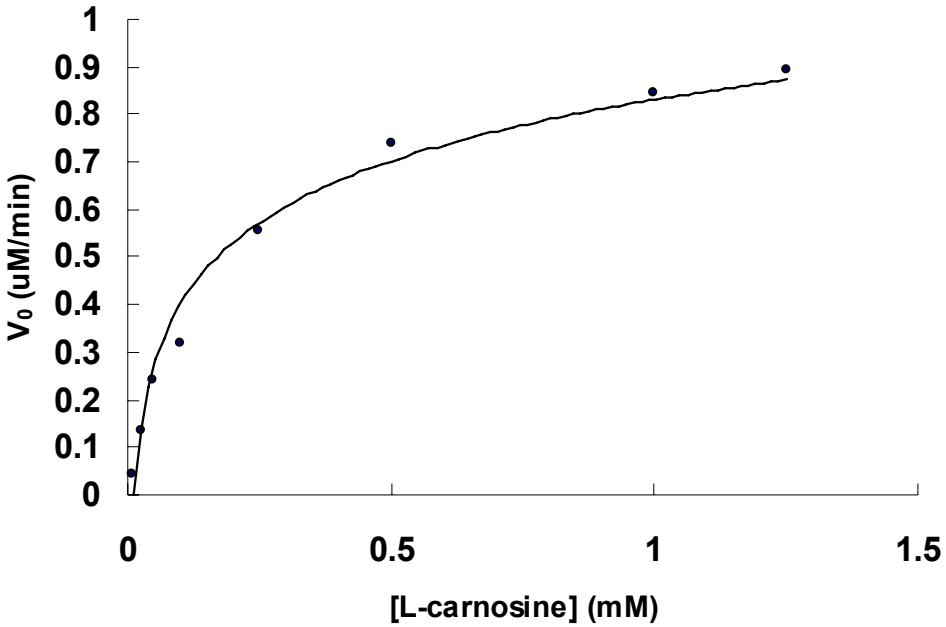

(b)

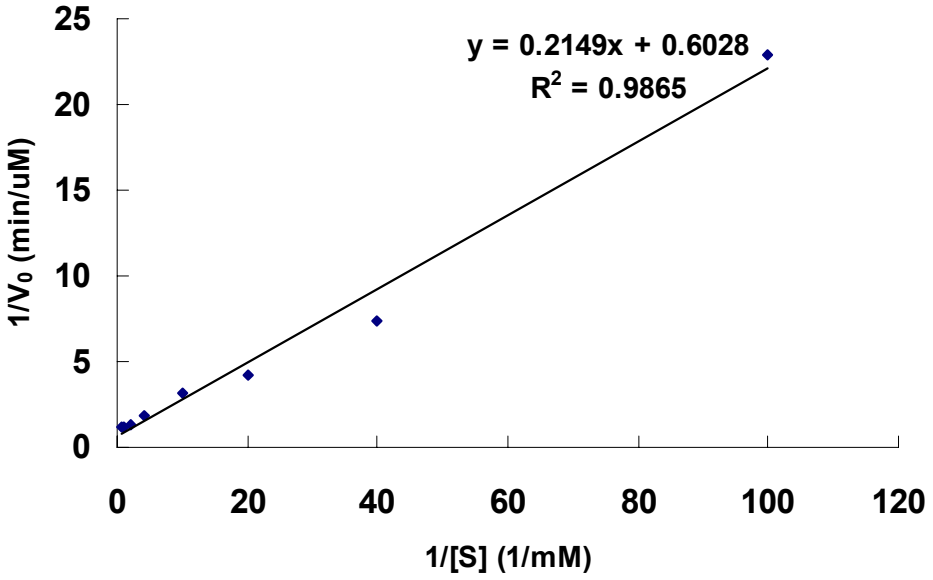

Fig. 7 Enzyme Kinetics of *V. alginolyticus* PepD (a) Michaelis-Menten plot for PepD catalyzed the hydrolysis of L-carnosine in 50 mM Tris-HCl, pH 6.8 at 37 **ºC**. (b) Lineweaver-Burk plot calculated from the respective Michaelis-Menten plot.

3.5 Site-directed mutagenesis analysis of *Vibrio alginolyticus pepD*

In order to identify the putative active site of PepD, site-directed mutagenesis analysis was performed to investigate the essential amino acids. Recent studies reported that the active site residues of enzymes in M20 family were almost conserved.[55, 58] Pep V, the first dinuclear dipeptidase with carnosine-hydrolyzing enzymatic activity protein in M20 family has been crystallized in 2002. PepD showed 20.9% identity and 34.3% similarity with PepV based on the sequence alignment employing. Sequence alignment between PepD and PepV also revealed the proposed active site. Surprisingly, the active site residues of PepV were almost conserved in PepD. These residues, including His80, Asp119, Glu150, Asp173, and His461 were expected for the metal binding, whereas Asp82 and Glu149 were expected for the catalysis (Fig. 8).

It was notable that the conserved residue Asp119 of PepD was equal to the adjacent residue Asp 120 of PepV that is the adjacent residue next to its metal binding residue Asp119. It is common that aspartic acid residue exhibited the metal binding role extensively at the active site of the enzymes in M20 family. The PepV peptide group between the bridging Asp119 and the adjacent residue Asp120 exhibited a *cis*-conformation to affect the binding of the metal, whereas the Asp 119 from PepD might be considered to associate with two zinc ions simultaneously. The *cis*-conformation is thought to be necessary to force the important zinc bridging carboxylate into the correct geometry as described in 1.7. Therefore, the residue Asp119 of PepD may play a more important role on metal binding hence involve in the enzymatic activity. In the study Asp119 and another proposed catalytic residue Glu149 were initially investigated by site-directed mutagenesis.

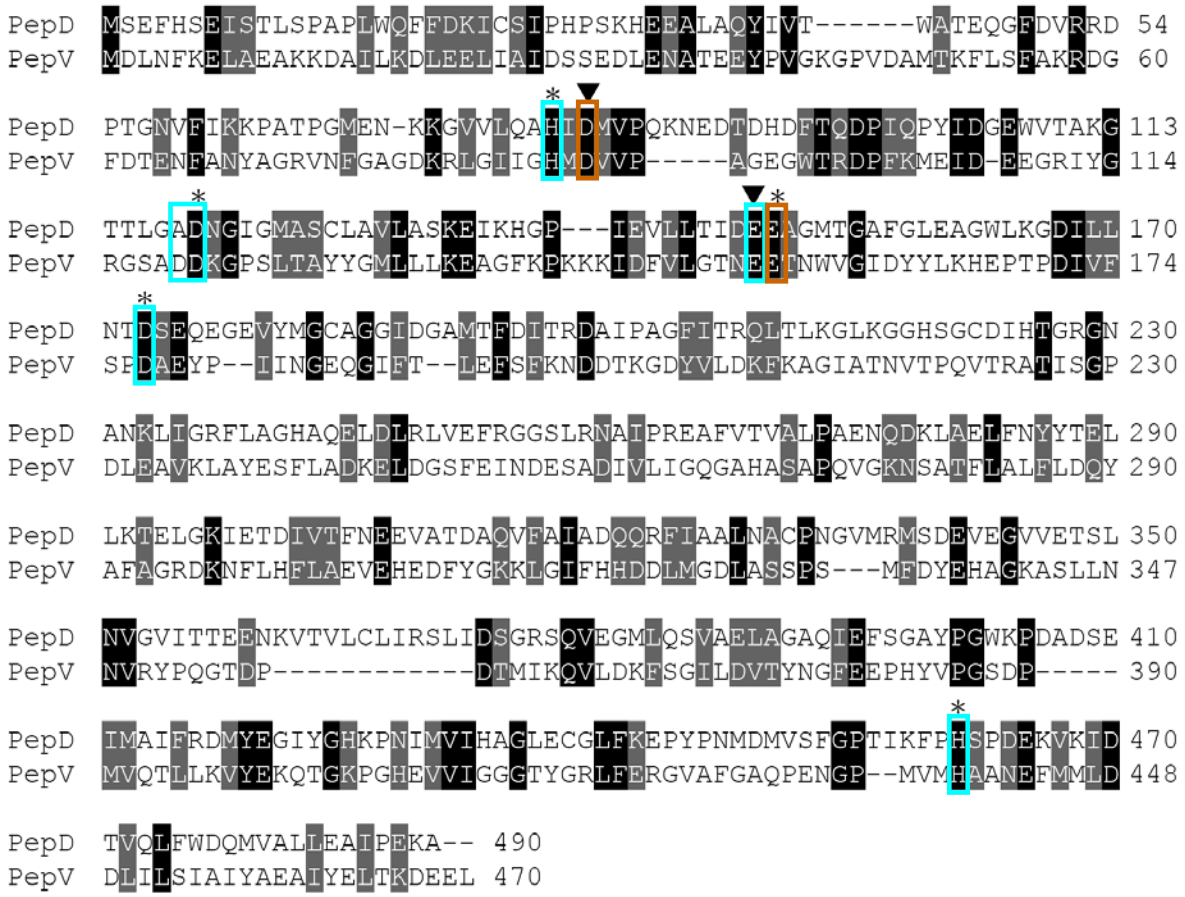

Fig. 8 Multiple sequence alignment with PepD and PepV

Identical and conserved amino acids between the sequences are marked in black and gray, respectively. Dashed lines indicate the gaps introduced for better alignment.

▼ Proposed active site residues : Asp82 ,Glu149

∗ Proposed metal ion binding residues : His80, Asp119,Glu150, Asp173, His461

The desired mutants were generated by QuickChange site-directed mutagenesis kit as described in 2.9 and the mutant plasmids were transformed into *E. coli*. BL21(DE3)pLysS to express the mutant proteins. Following the same purification experimental procedure of *V. alginolyticus* wild-type PepD, the mutant PepD proteins were carried out with 20 mM Tris-HCl pH 6.8 buffer containing 150 mM imidazole by Ni-NTA column chromtography. The purified wild-type and mutant PepD proteins showed the same molecular weight about 55 kDa on SDS-PAGE (Fig. 9~10.).

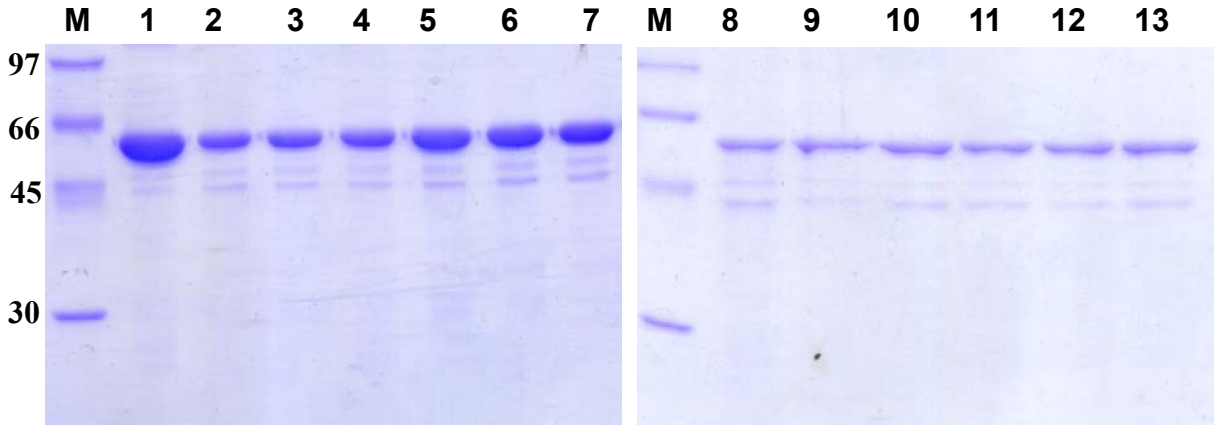

Fig. 9 SDS-PAGE (12%) of purified wild-type and mutant proteins of D119.

Lane M:LMW protein marker; Lane 1:PepD wild type; Lane 2:PepD D119E mutant; Lane 3:PepD D119M mutant; Lane 4:PepD D119L mutant; Lane 5:PepD D119I mutant; Lane 6:PepD D119 R mutant; Lane 7:PepD D119F mutant; Lane 8:PepD D119A; Lane 9:PepD D119S mutant; Lane 10:PepD D119T mutant; Lane 11:PepD D119C mutant; Lane 12:PepD D119P mutant; Lane 13:PepD D119N mutant

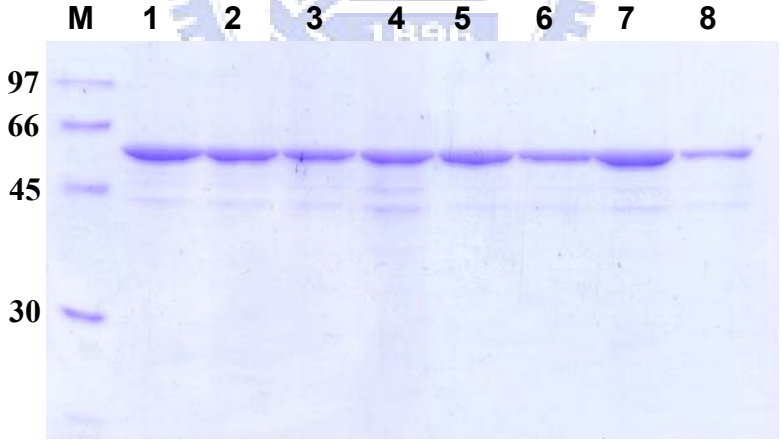

Fig. 10 SDS-PAGE (12%) of purified wild-type and mutant proteins of E149.

Lane M:LMW protein marker; Lane 1:PepD wild type (WT); Lane 2:PepD E149A mutant; Lane 3:PepD E149D mutant; Lane 4:PepD E149G mutant; Lane 5:PepD E149S mutant; Lane 6:PepD E149Q mutant; Lane 7:PepD E149H mutant; Lane 8:PepD E149R mutant

In *E. coli*, PepD was indicated as a homodimer in native sate.[29] To observe the native form of PepD in *V. alginolyticus*, the wild-type and mutant PepD derivatives were analyzed with 7.5% Native-PAGE analysis (Fig. 11) A major band with molecular mass near 66 kDa of the protein marker was observed. Interestingly, several weak bands were also examined on the Native-PAGE of the wild-type and mutant PepD. Therefore, it was proposed that PepD in *V. alginolyticus* might exist in many forms in the native state. The major band with molecular weight about 66 kDa might be the monomer that PepD tended to form in its native state. The minor weak band with molecular weight near 140 kDa might be the homodimer form. To ensure the native form of PepD in *V. alginolyticus*, the Westeewrn blotting, that examining a clear band on the film was carried out using anti-PepD mAb (Fig. 12). Besides, Analytical Ultracentrifugation (AUC) was also used to confirm the result of Native-PAGE analysis and Western blotting (Fig. 13). However, the calculated molecular weight from sedimentation coefficient (*s*) indicated that PepD preferred to form homodimer in its native state. The calculated molecular weight of denatured PepD protein was as a control comparing to the molecular weight of wild-type PepD protein (Fig. 14).

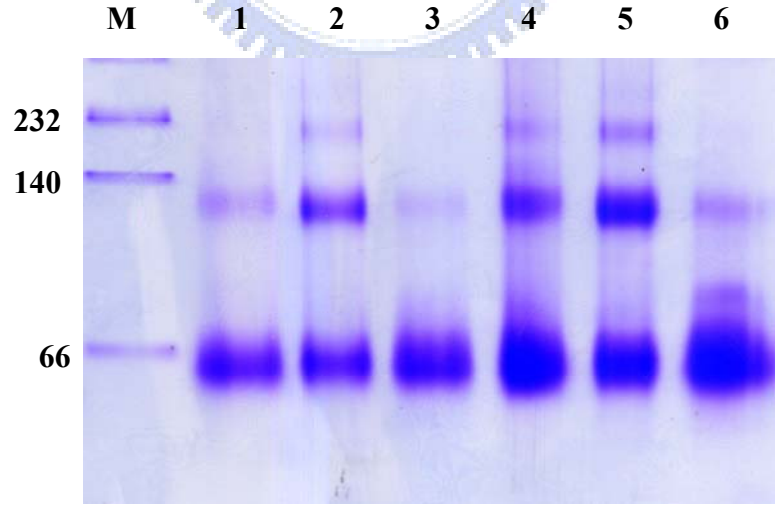

Fig. 11 Nativ-PAGE (10%) analysis of purified PepD wild-type and mutant proteins Lane M:HMW Native protein marker; Lane1: PepD wild-type(20 μL); Lane 2:PepD D119E mutant (20 μL); Lane 3:PepD E149D mutant (20 μL); Lane 4:PepD wild-type (40 μL); Lane 5:PepD D119E mutant (40 μL); Lane 6:PepD E149D mutant (40 μL)

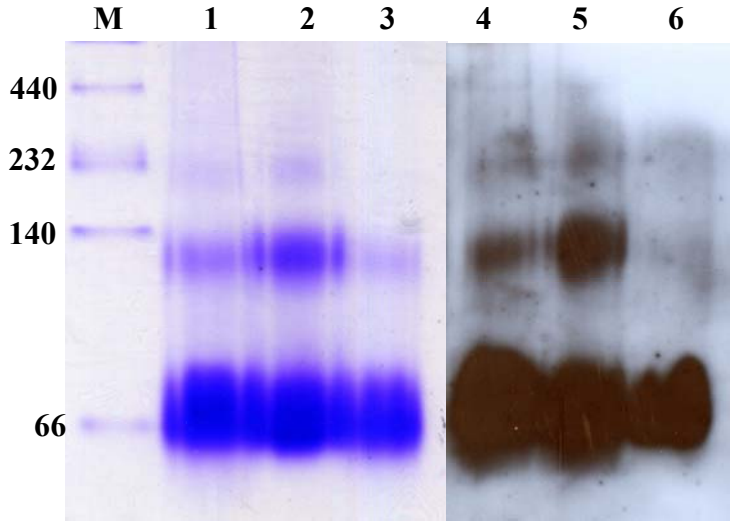

Fig. 12 Western blotting analysis of purified PepD wild-type and mutant proteins

Lane M:HMW Native protein marker; Lane 1:PepD wild-type; Lane 2:PepD D119E mutant; Lane 3:PepD E149D mutant; Lane 4:PepD wild-type; Lane 5:PepD D119E mutant; Lane 6:PepD E149D mutant

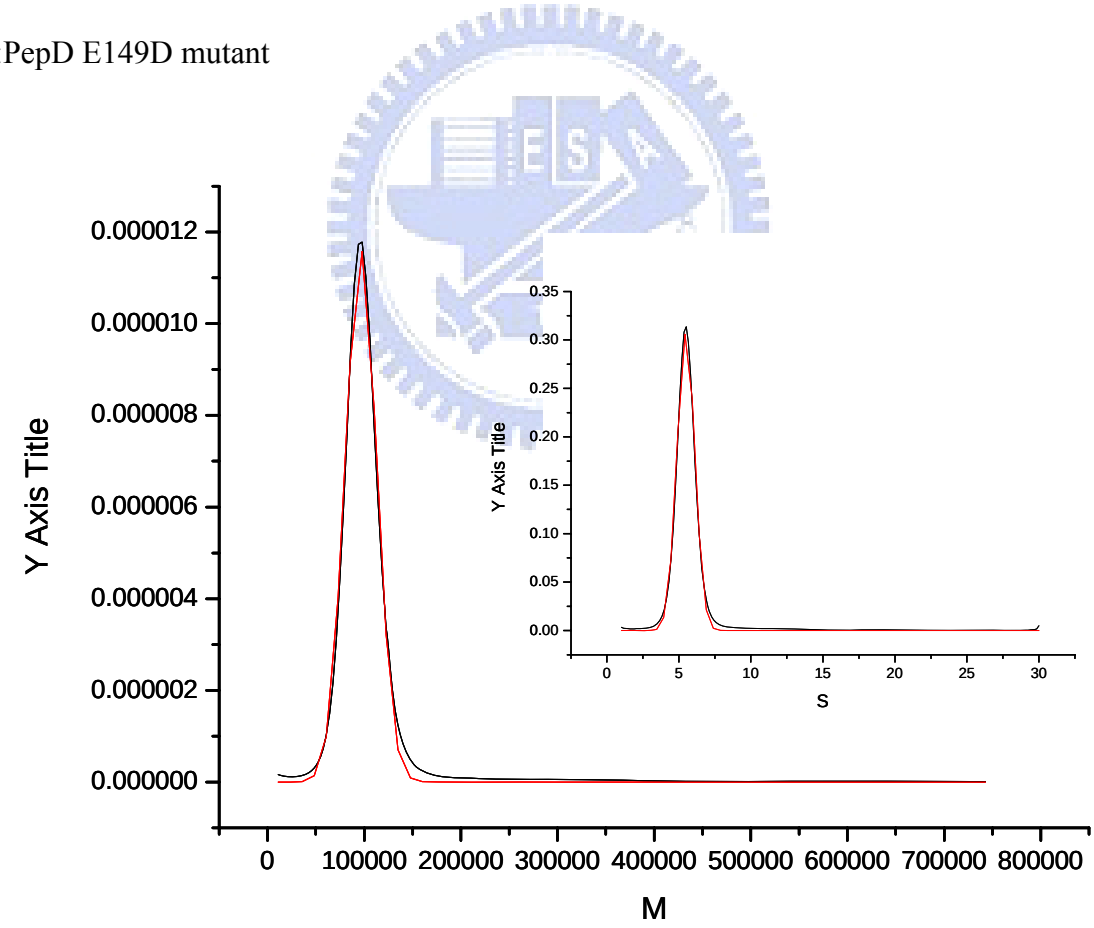

Fig. 13 Analytical ultracentrifugation determination of PepD protein

The molecular weight of *V. alginolyticus* PepD is 53548.8 g/mol. The calculated molecular weight from sedimentation coefficient (*s*) is about 96817.977 g/mol.

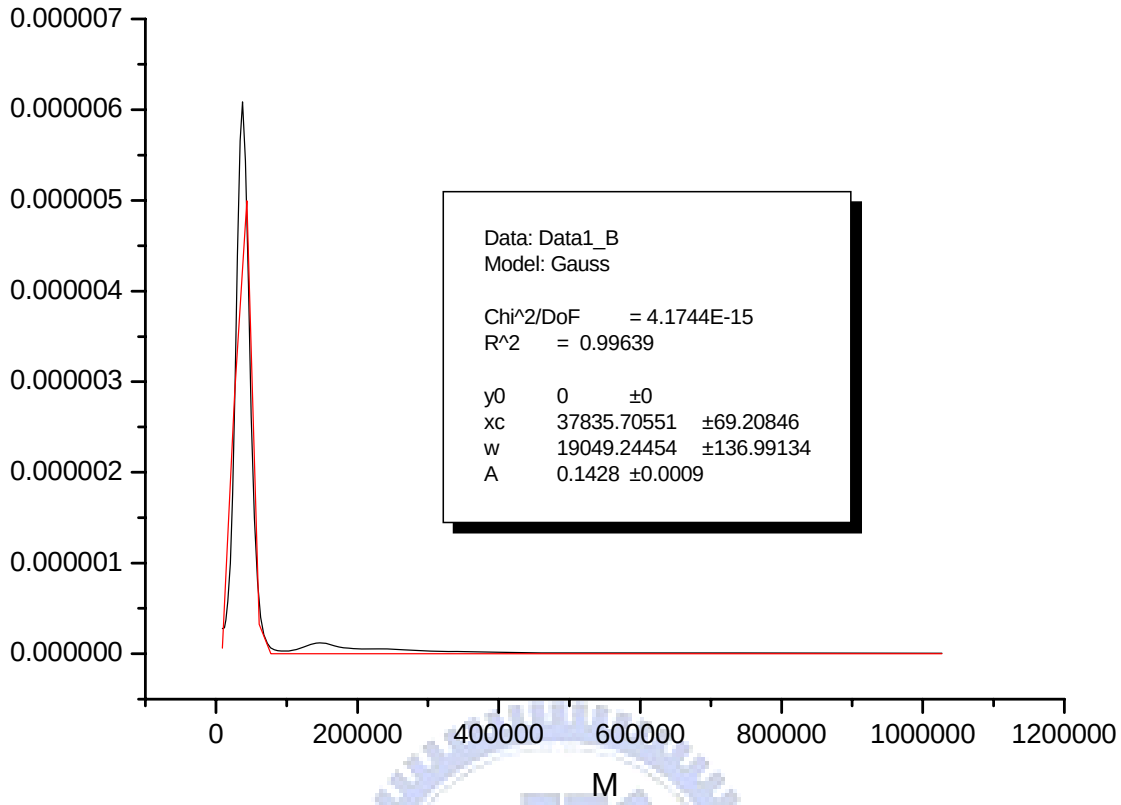

Fig. 14 Analytical ultracentrifugation determination of denatured PepD protein

The calculated molecular weight of denatured PepD protein from sedimentation coefficient (*s*) is about 37835.71 g/mol.

3.6 Enzyme kinetic of the mutant PepD

The enzyme activity of the mutant PepD was performed with hydrolyzing L-carnosine in the same experimental process of the wild-type PepD, as described in 2.6. Compared to the wild-type PepD, no apparent activity could be detected among almost all mutanted-PepD except the E149D mutant (Fig. 15).

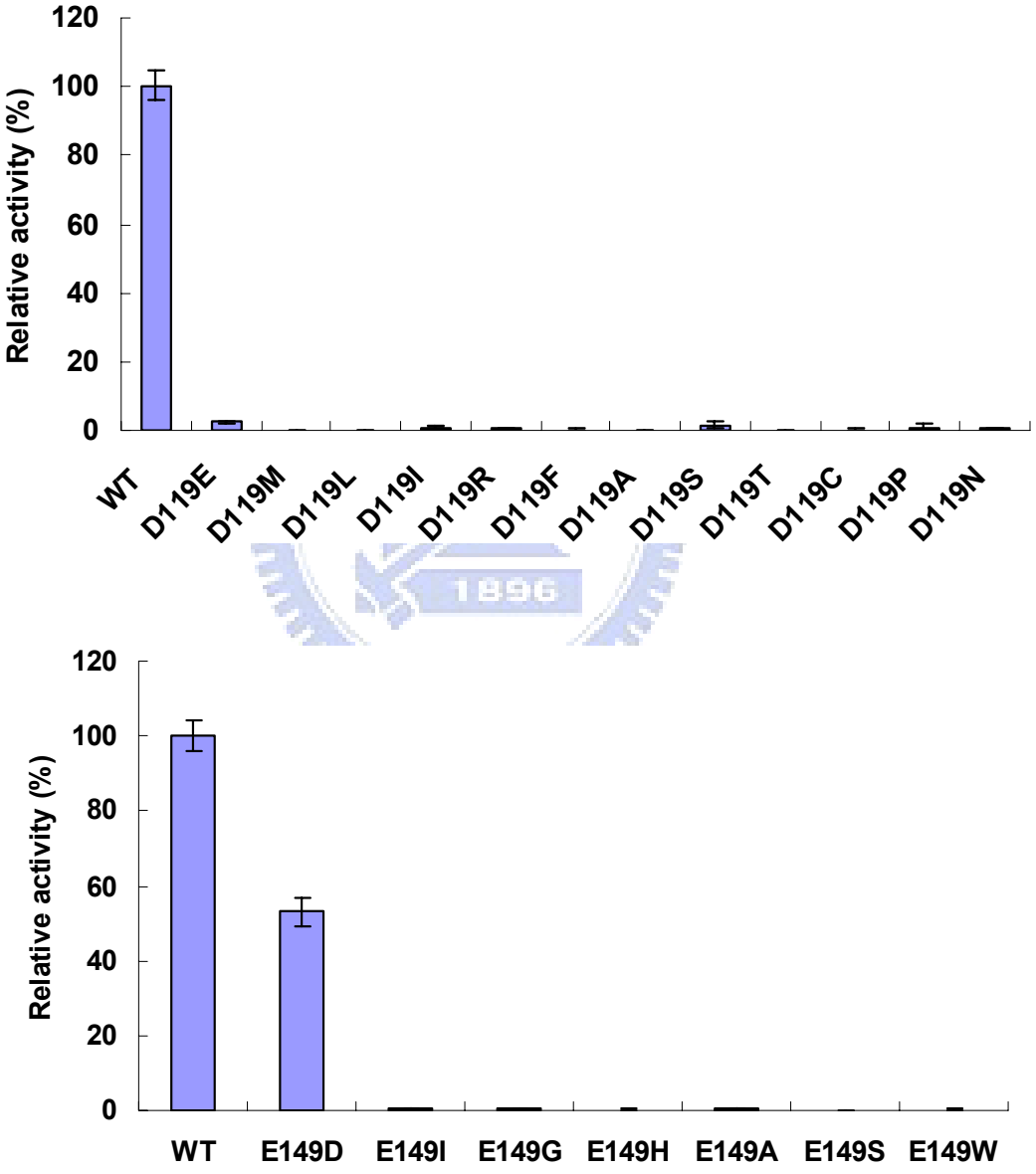

Fig. 15 Enzymatic activities of wild-type and mutant PepD on L-carnosine. Purified wild-type and mutant PepD proteins were subjected to the activity assay on L-carnosine as a substrate. The wild-type activity was defined as 100%

Moreover, the enzyme kinetic of the mutants to determine the V_{max}, K_m and K_{cat} values, and compared to that of the wild-type PepD. The V_{max} and K_m values of the E149D mutant (2 μg, 0.186 μM) for L-carnosine calculated from the respective Lineweaver-Burk plot were 1.1 μM/min and 0.53 mM (Fig. 16).

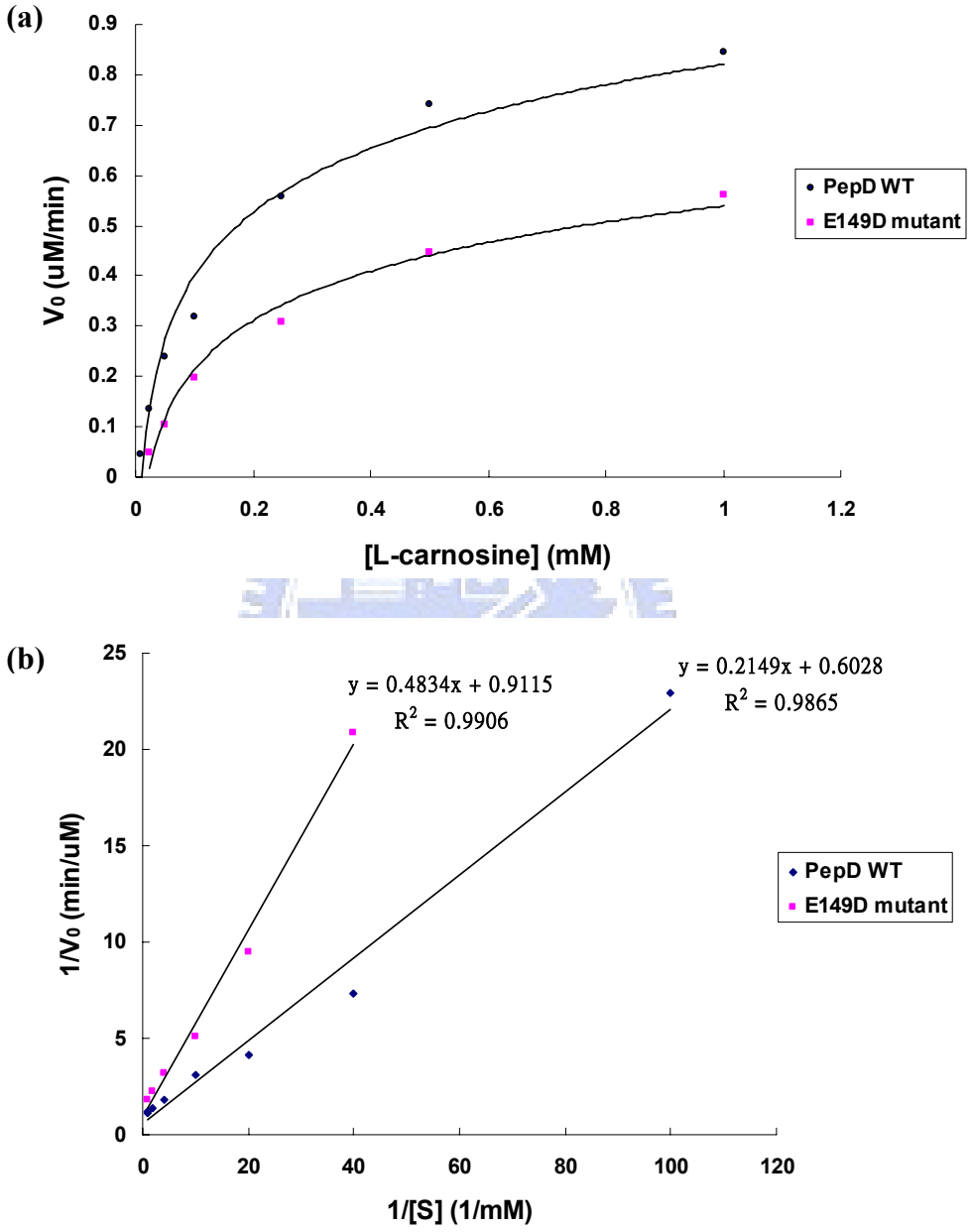

Fig. 16 Enzyme kinetics of wild-type and mutant PepD (a) Michaelis-Menten plot for wild-type and E149D mutant which catalyzed the hydrolysis of L-carnosine in 50 mM Tris-HCl, pH 6.8 at 37 ºC. (b) Lineweaver-Burk plot calculated from the respective Michaelis-Menten plot.

Therefore, the turnover number (k_{cat}, $k_{cat} = V_{max}/[E]_T$) of E149D for L-carnosine in 50 mM Tris-HCl, pH 6.8 at 37 ºC is 5.9 min^{-1} and the catalytic efficiency (k_{cat}/K_m) is 0.186 $mM^{-1}s^{-1}$. Moreover, no activity at all could be detected for the D119E mutant (Table 6).

Table 6. Kinetic Parameters for the hydrolysis of L-carnosine at 37 ºC and pH 6.8 of wild-type and mutant *V. alginolyticus* PepD

PepD variant	k_{cat} (min^{-1})	K_m (mM)	k_{cat}/K_m ($mM^{-1}s^{-1}$)
Wild-type	8.6	0.36	0.398
E149D	5.9	0.58	0.186
D119E	ND	ND	ND

3.7 The secondary structure of *Vibrio alginolyticus PepD*

There is a common problem that the mutants created by using site-directed mutagenesis techniques might cause global conformational changes that inactivate the protein. Circular dichroism (CD) spectrum analysis can give information on the secondary structure content of protein. The α-helix, β-sheet, and γ-turn are three main types of secondary structure in proteins. The different types of regular secondary structure in proteins would give rise to characteristic CD spectra in the far UV.[63] CD spectroscopy was performed on the purified PepD WT and mutant proteins to prove that the loss or decreasing activity of the mutants were not due to the change of secondary structure of protein. The far-UV CD spectra of the wild-type and mutant PepD spectra were similar (Fig. 17).

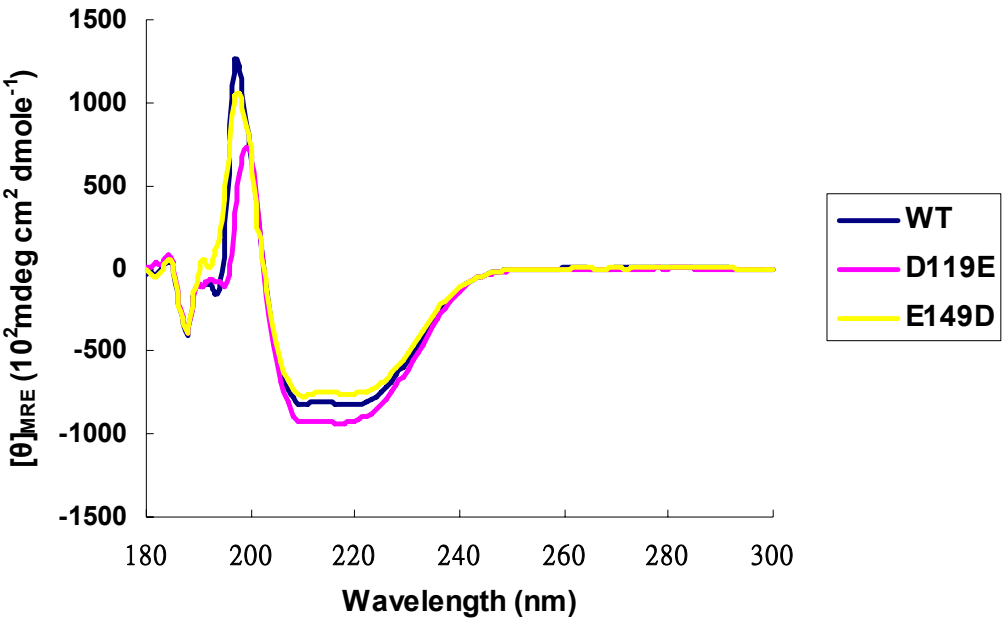

Fig. 17 The CD spectra of *Vibrio alginolyticus PepD* wild-type and mutant proteins.

The predict percentages of secondary structure from CD spectra also suggested that the secondary structure of wild-type and mutant PepD were almost the same (Table 7). Accordingly, PepD mutants did not produce the structural misfolding dramatically and the influence on its activity might come from the mutated-inducing enzymatic activity change.

Table 7. The secondary structure content of wild-type and mutant *V. alginolyticus* PepD

	α-helix (%)	β-sheet (%)	random coil (%)
WT	**31**	**11**	**58**
D119E	**31**	**10**	**58**
E149D	**30**	**14**	**57**

(http://www.embl-heidelberg.de/~andrade/k2d/)

3.8 Structure features of *Vibrio alginolyticus PepD*

To predict the active site residues of *V. alginolyticus* PepD, the computational analysis was also carried out through homology modeling analysis. The PepD model was obtained with *L. delbrueckii* PepV as the template, and the generated PepD structure is quite similar to PepV structure (Fig. 18).

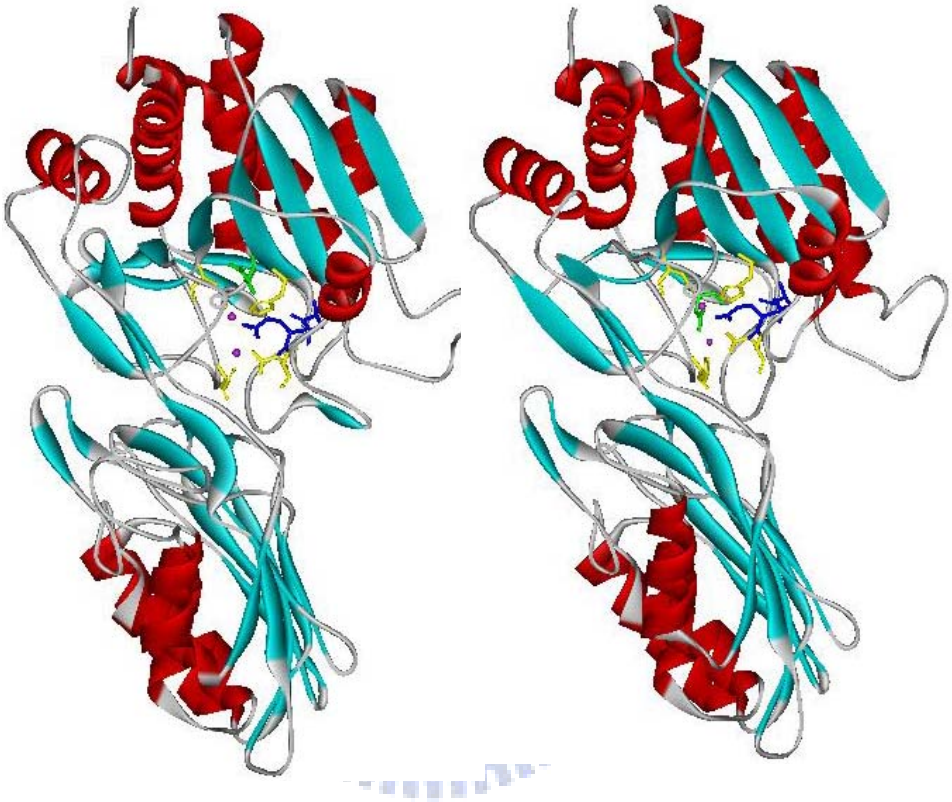

Fig. 18 Three-dimensional ribbon of the crystal structure of PepV(right) and the generated PepD(left) model based on PepV. The PepD catalytic domain has a fold similar to the dinuclear carnosine-hydrolyzing enzyme PepV. The structure predicted two zinc ions at the catalytic pocket center which were held by five metal binding residues (yellow) including the adjacent residue Asp119 (light green). The residues for catalytic (blue) were quite similar.

Apparently, based on the results of sequence alignment, activity assay, and homology modeling, seven residues including His80, Asp119, Glu150, Asp119, Asp173, His461 were thought to be involved in the active site of *V. alginolyticus* PepD crucial for associating with zinc ions , and Asp82 and Glu149, two catalytic residues. Moreover, the superimposition of

PepV active site residues with PepD revealed that the predicted active site residues of PepD were almost equivalent to that of PepV (Fig. 19).

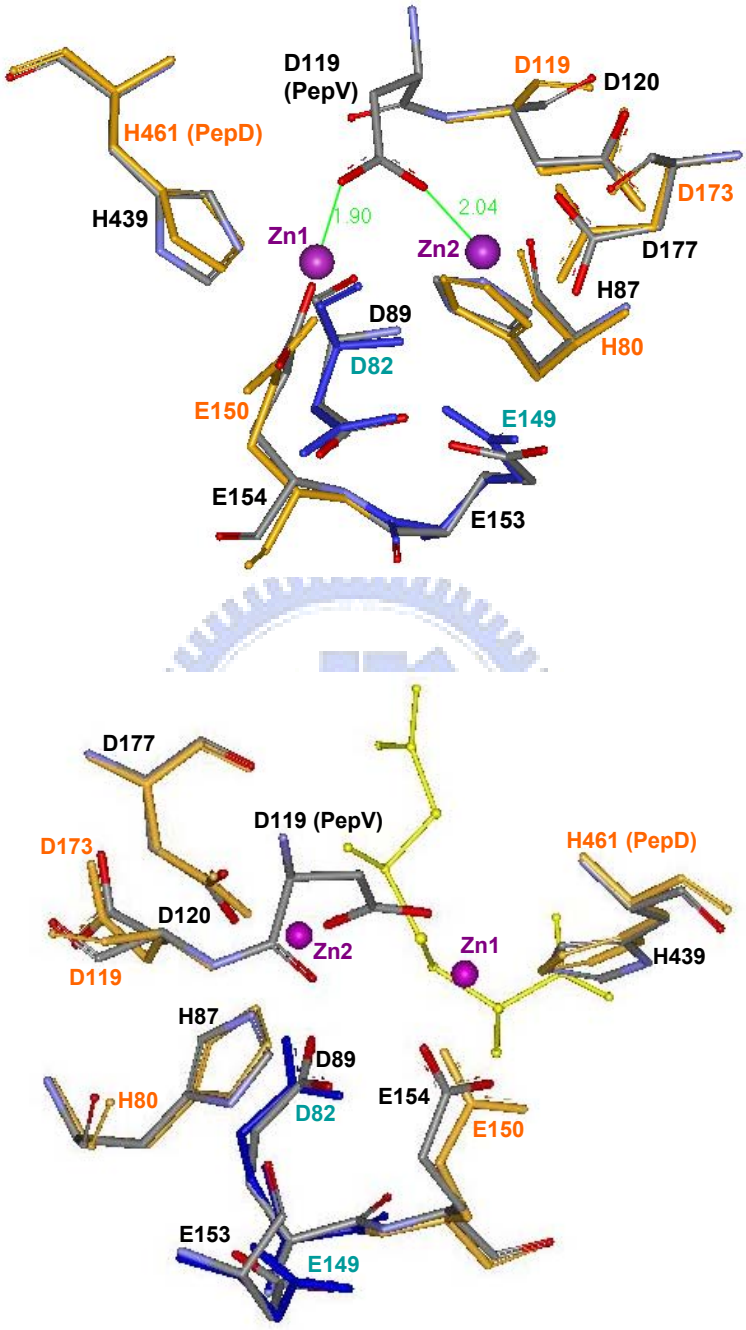

Fig. 19 Stereo view of PepD (blue) superimposed with the active site residues of PepV. The gray sticks are residues of PepV, and the orange sticks (metal binding) and the blue sticks (catalytic) are residues of PepD. The predicted metal binding residues of PepD are almost equivalent to that of PepV. The yellow stick is the phosphinic inhibitor AspΨ[PO_2CH_2]AlaOH of PepV.

It was considered that the active site residues of enzymes in M20 family were almost conserved. Carboxypeptidase G_2 (CPG_2), the first dinuclear dipeptidase with available crystal structure in M20 family, was proven to cleave the the *C*-terminal Glu from folic acid and folate analogs.[58] The structure homology models showed that the catalytic domain of PepV has a similar folding to the CPG_2 and the active sites residues of PepV were fully conserved in CPG_2.[55] In the other hand, the sequence of PepD showed 19.3% identity and 34.2% similarity with CPG_2. To determine the putative catalytic domain of PepD, the sequence alignment and superimposition of CPG_2 active site residues with PepD was also performed. The result revealed that the predicted active site residues of PepD were almost equivalent to that of PepV and CPG_2 (Fig. 20, 21), only the residue Asp119 of PepD displayed a notable difference in this model. However, loss of enzymatic activity of PepD D119 mutant indicated that this residue might play an important role for the PepD mediated cleavaging reaction.

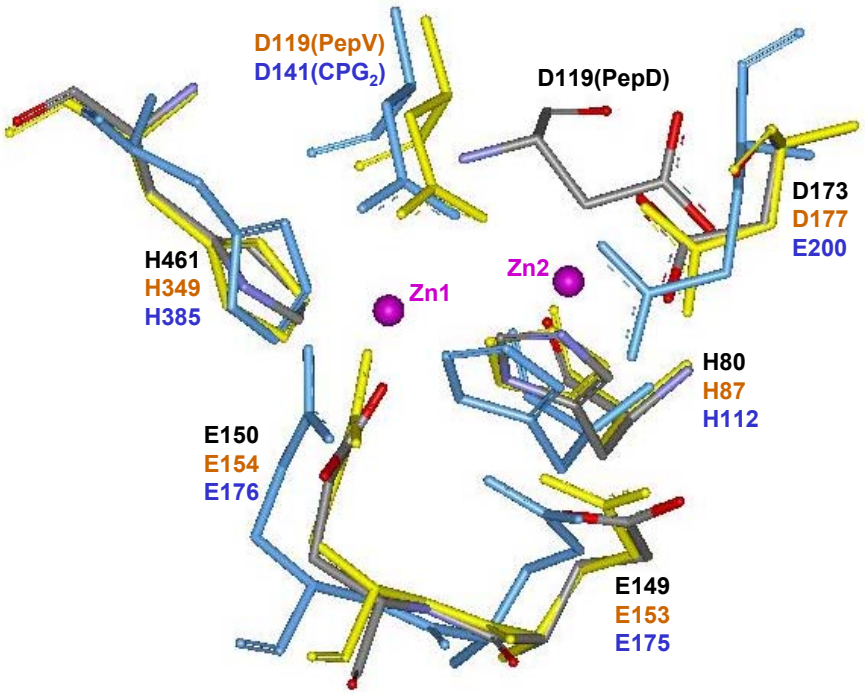

Fig. 20 Local view of PepD superimposed with the active site residues of PepV and CPG_2. The residues were respectively colored in gray, yellow and blue for PepD, PepV and CPG_2. The active site residues were almost equivalent. The zinc binding residue Asp173 in PepD and equivalent aspartic acid in PepV was substituted by glutamic acid in CPG_2.

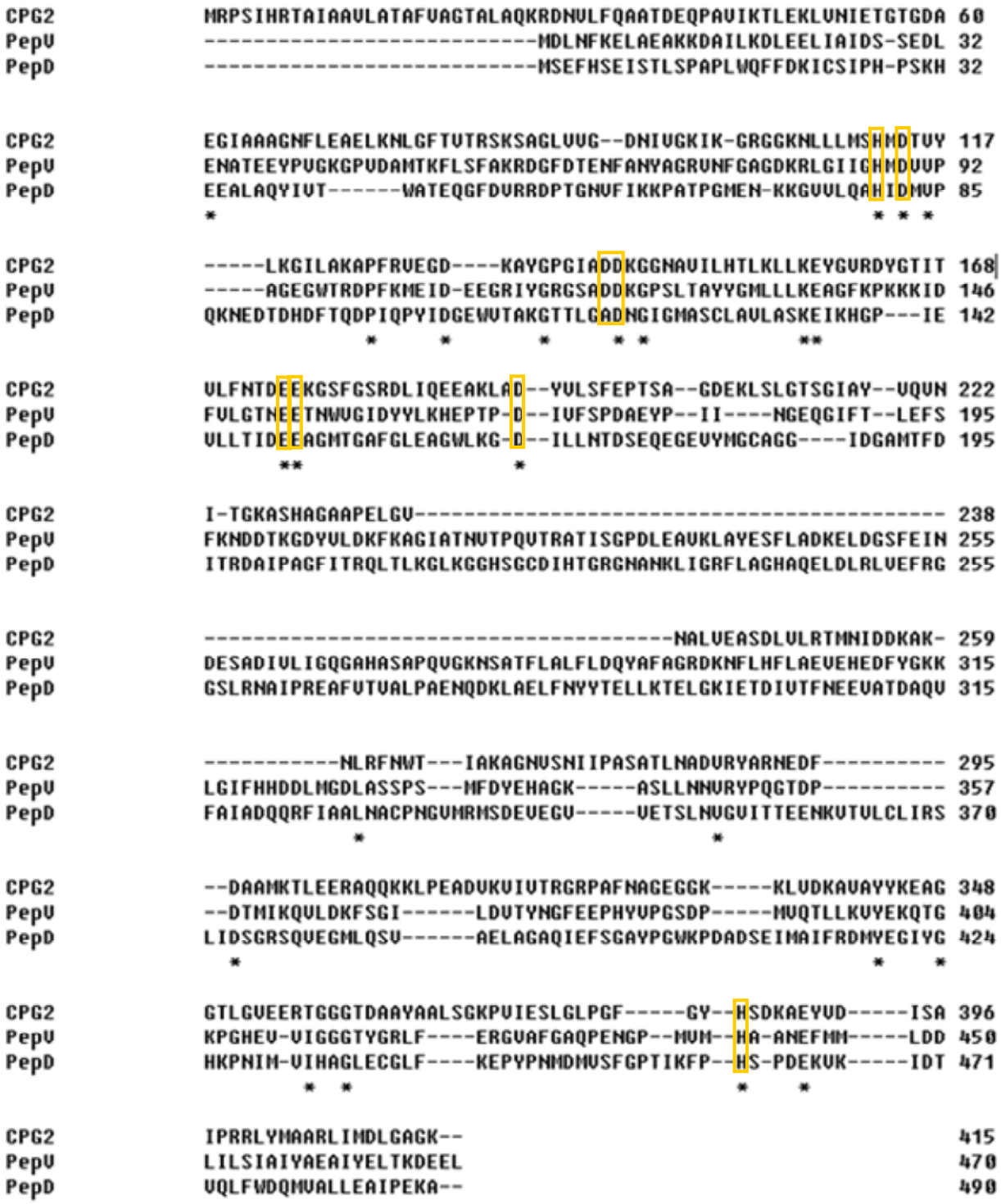

Proposed active site residues : Asp82 ,Glu149

Proposed metal ion binding residues : His80, Asp119,Glu150, Asp173, His461

Fig. 21 Multiple sequence alignment with CPG_2, PepV and PepD

3.9 Crystallization of *Vibrio alginolyticus* PepD

The *V. alginolyticus* PepD crystals were obtained by using hanging drop technique as described in 2.12. Hanging drops were formed by mixing 1 μL of 10 mg/mL enzyme solution with 1 μL crystallization reagent. The crystals were yielded at 20 ºC in two weeks under two condition: Crystallization reagent was composed of (a) 20% PEG-4000, 10% isopropanol, 0.1 M Na-HEPES, pH 7.5 (b) 28% PEG-400, 0.1 M Na-HEPES, 0.2 M $CaCl_2$, pH 7.5 (Fig. 22). The crystals diffraction was 2.7 Å at best, but the quality of this data collection was not useful for phasing. Therefore, further modification of the precipitation condition should be undertaken and hope to obtain the high-resolution crystals for structure determination in the future.

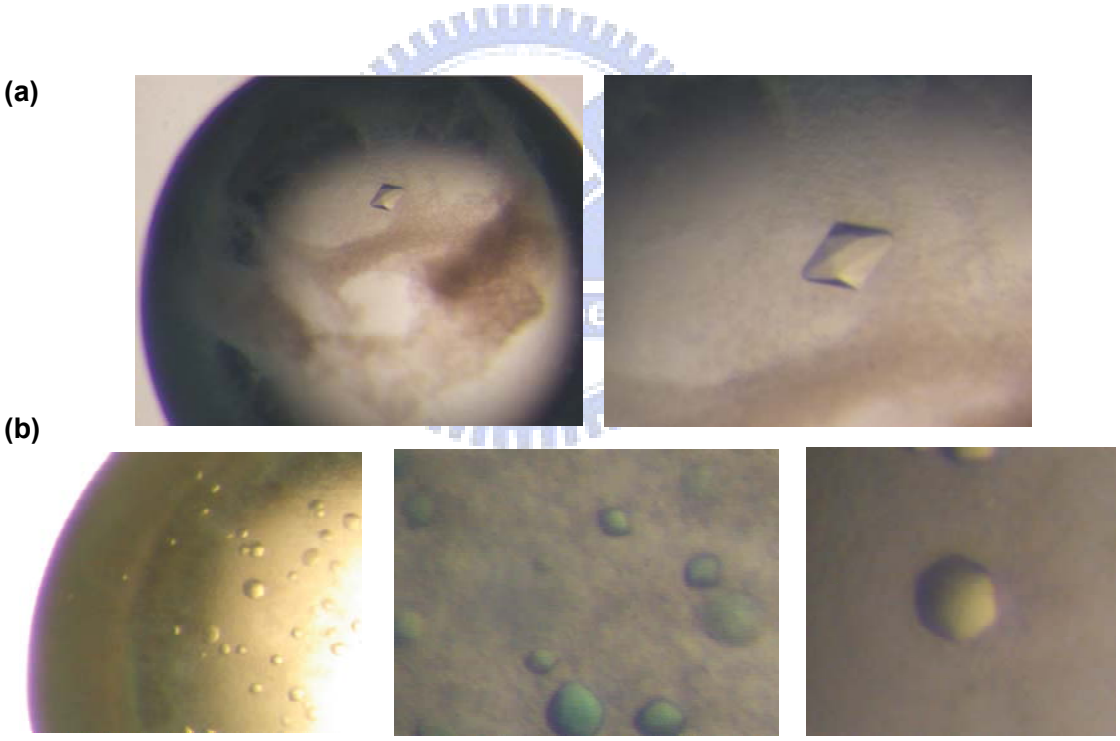

Fig. 22 The *V. alginolyticus* PepD crystals were grown at 20 ºC in two condition: (a) 20% PEG-4000, 10% isopropanol, 0.1 M Na-HEPES, pH 7.5 (b) 28% PEG-400, 0.1 M Na-HEPES, 0.2 M CaCl2, pH 7.5

Chapter 4 Discussion and conclusion

In this study, *V. alginolyticus* PepD which identified as a member of metallopeptidase M20 family and considered as an aminoacylhistidine dipeptidase was being investigated. The recombinant PepD of *V. alginolyticus* with a His-tag on *N*-terminus was successfully expressed and purified with high purity. Based on the SDS-PAGE analysis, the molecular mass of PepD is about 55 kDa near to the calculated molecular mass of 53.6 kDa. and is also similar to that of previously identified *E. coli* PepD.[29]

The *V. alginolyticus* PepD enzymatic activity was performed on L-carnosine-hydrolyzing, which was similar to that exhibited by all of the known PepD. It could hydrolyze the unique dipeptide L-carnosine (β-Ala-L-His), which has potential neuroprotective function in brain and could act as an antioxidant or antiglycation agent. The substrate specificity of PepD in *V. alginolyticus* was also identified in this study. It could degrade a large number of Xaa-His dipeptides besides brain-specific dipeptide like GABA-His. The amino group in α or β position of *N*-terminus residue did not affect the recognition and hydrolysis of dipeptide. However, with the more tendency for α-Ala-L-His than L-carnosine as substrate was first identified in bacterial PepD, whereas the same result could also be observed in human cytosolic nonspecific dipeptidase (CN2).[42] Several Xaa-His dipeptides including Val-His, Leu-His, Tyr-His, Ile-His, His-His and Ser-His were superior over carnosine as substrates for degradation and the enzyme also could hydrolyze Gly-His with good activity but had no apparent activity on β-Asp-L-His. Therefore, we preliminary assumed that this enzymatic activity on Xaa-His dipeptides is dependent on the charge of Xaa amino acid. The His-Xaa dipeptides including His-Ile or His-Val, as well as tripeptides containing histidine in the central part or *C*-terminal position were not degraded, indicating that *V. alginolyticus* PepD is a Xaa-His dipeptidase in activity. The study of substrate specificity on Xaa-His dipeptides was first carried out in bacterial aminoacylhistidine

dipeptidase, but had already been identified in mammals.

The kinetic values including k_{cat} *or* k_{cat}/K_m, were compared with the mammal aminoacylhistidine dipeptidases while lacking of the related reports for the bacterial PepD and PepV. The K_m value and catalytic efficiency (k_{cat}/K_m) of *V. alginolyticus* PepD for L-carnosine were 0.36 mM and 0.398 $mM^{-1}s^{-1}$, respectively. As compared with that of human carnosinase (CN1) (K_m 1.2 mM and k_{cat}/K_m 8.6 $mM^{-1}s^{-1}$), PepD catalyzes at a relative low efficiency. However, the K_m value of *V. alginolyticus* PepD was lower than PepD of *Escherichia coli* K-12 (2 to 5 mM) [30] indicated a relatively higher interaction of *V. alginolyticus* PepD with its substrates. Based on the result of higher hydrolysis rate on α-Ala-L-His than β-Ala-L-His as the substrate, PepD could have other more suitable dipeptide substrate for degradation or even another totally different enzymatic activity. Moreover, the inhibitiory effect of bestatin on L-carnosine hydrolysis by PepD will be investigated.

According to the result of sequence alignment between PepV and PepD, the active site residues were almost conserved. We predicted that there are five putative metal binding residues, His80, Asp119, Glu 150, Asp173, and His461, and two catalytic residues, Asp82 and Glu149 in the enzymatic active site cavity. The conservation of the active site residues suggests that the hydrolytic mechanism of PepD and PepV might be closely related. The PepD mutants created by site-directed mutagenesis on putative metal binding residue Asp119 resulting in losing the activities but without changing the secondary structure with CD spectra analysis. It revealed that this residue might be involved in the metal binding for the dramatically affecting enzymatic activity. There were no detectable zinc ions in the D119E mutant crystal by X-ray diffraction, preliminary confirming our hypothesis. We also investigated the residue of catalytic Glu149 for site-directed mutagenesis. Surprisingly,

almost the mutants lost the activities besides E149D that retained partial enzymatic activity. The similar spectra and the predict percentages of secondary structure from CD spectra compared with the wild-type PepD via CD spectra analysis confirmed that the similar secondary structure was existed in the mutant E149D. Based on this result, we suggested that changing of the putative catalytic residue glutamic acid to the aspartic acid with the same negative charge would keep the enzymatic ability to interact with the substrate.

To confirm our suggestion, the orientation relationship between the putative active site residues and zinc ions were investigated by molecular modeling. The carbonyl oxygen of the mutant D119E was far away from zinc ion to involve in the metal binding ability for the dramatically affecting enzymatic activity (Fig. 23).

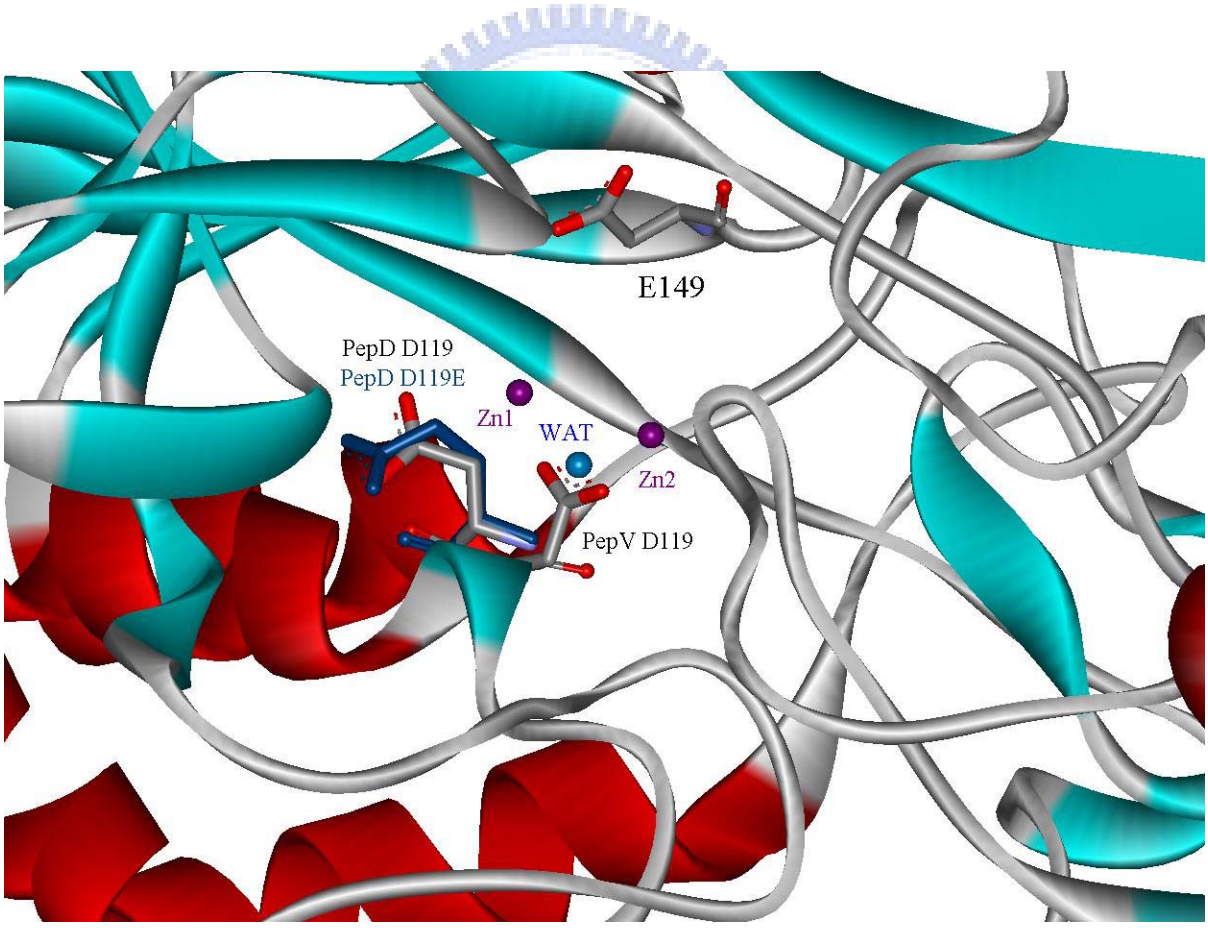

Fig. 23 Stereo view of orientation relationship between zinc ion and the putative metal binding residues Asp119.

The catalytic mechanism proposed that the bridging catalytic water attacks the carbonyl carbon of the scissile peptide bond to form a sp^3-orbital substrate-enzyme tetrahedral intermediate (Fig.24). The distant from the catalytic water to the carbonyl carbon of the mutant E149D was too far to from the substrate-enzyme tetrahedral intermediate that further involved in substrate binding ability and caused the mutant losing partial enzyme activity (Fig. 25).

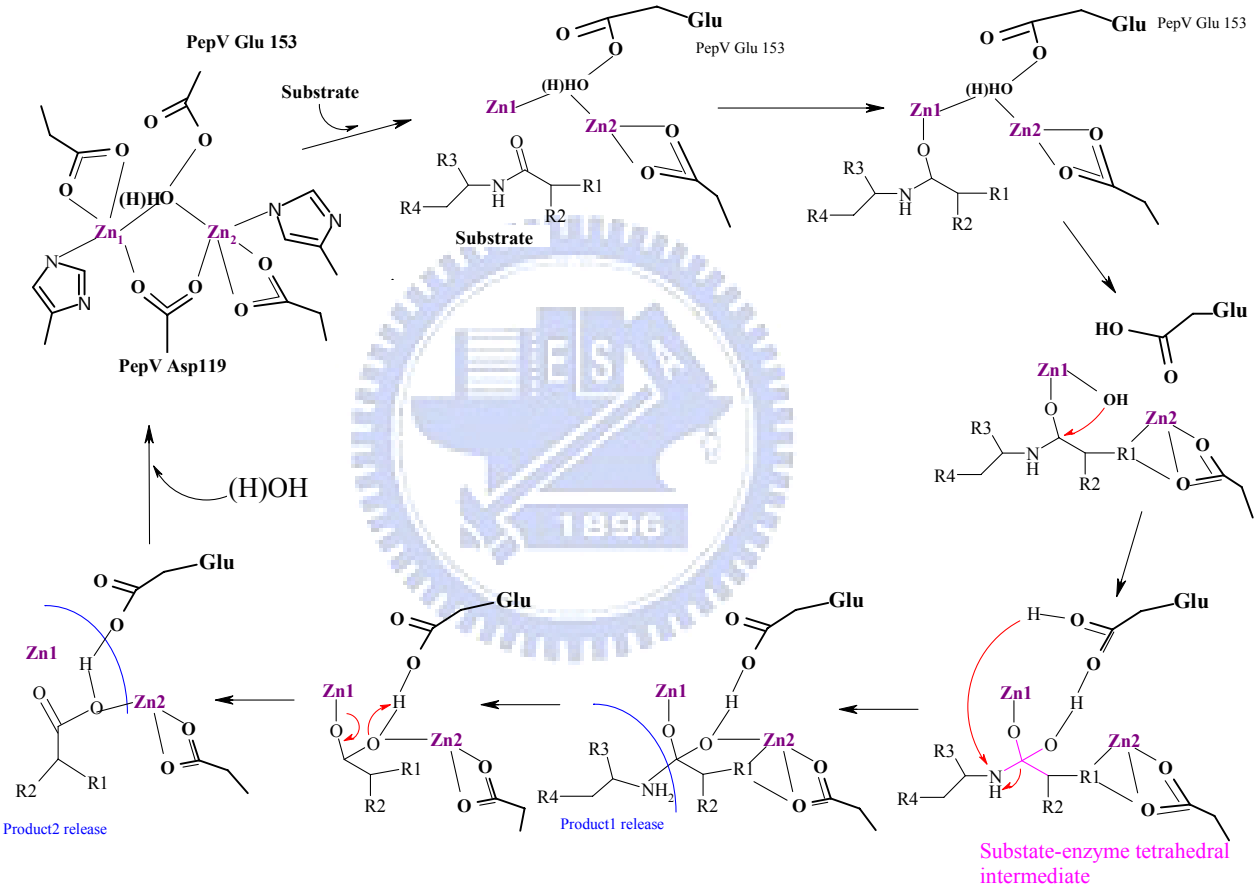

Fig. 24 Proposed catalytic mechanism for the hydrolysis of *N*-terminal amino acid residues. Proposed general mechanism for the hydrolysis of a peptide, catalyzed by a metallopeptidase with a co-catalytic active site where R1, R2, R3 are substrate side chains and R is an N-terminal amine or a C-terminal carboxylate.

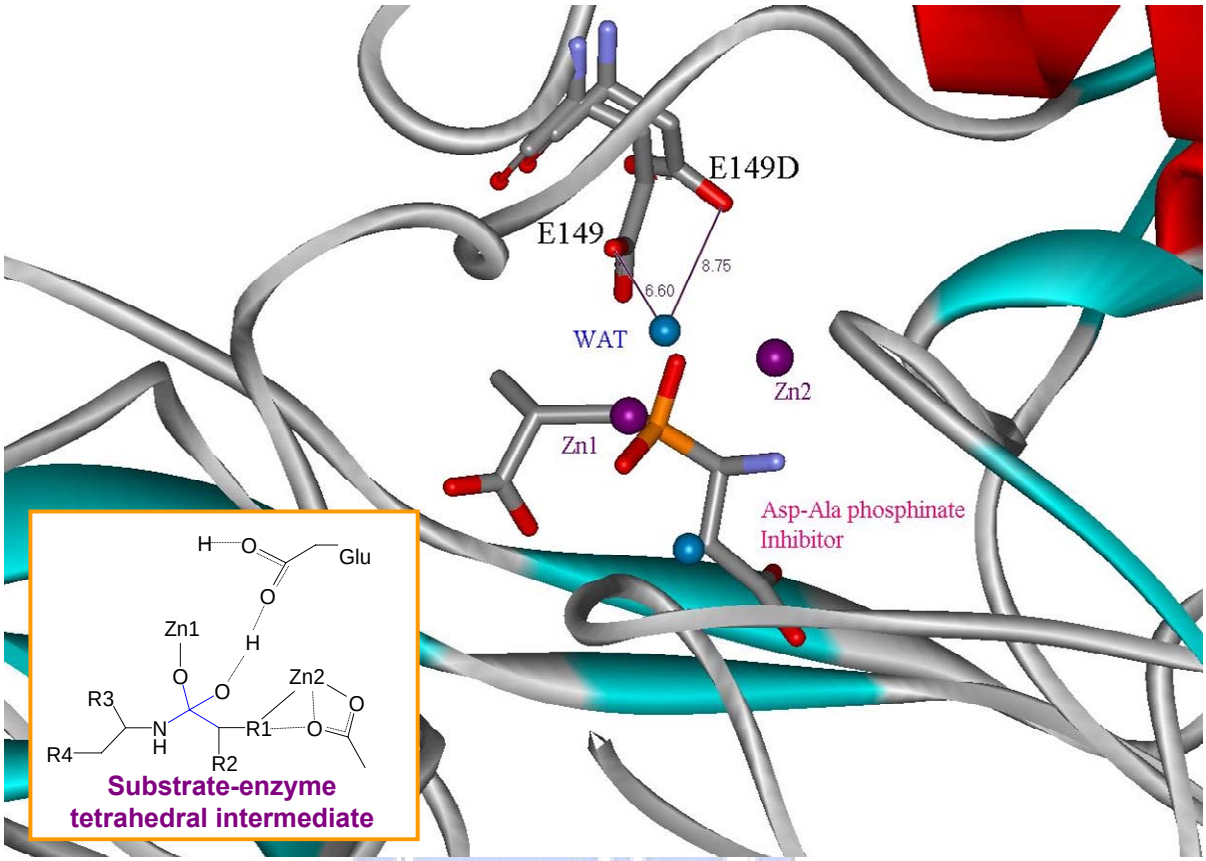

Fig. 25 Stereo view of orientation relationship between catalytic water and the putative catalytic residues Glu149.

The homology modeling structure of PepD was obtained from the *L. delbrueckii* PepV crystal structure with dizinc nuclear was quite similar. The putative residues for catalytic Asp82 and Glu149 of PepD were primarily superimposed on PepV Asp89 and Glu153 residues. Asp82 was conserved in all of the active enzymes from clan MH and considered to clamp the imidazolium ring of His80. Glu149 served as a general base in catalysis, whereas the water molecule was bridged by two zinc ion acting as the attacking hydroxyl ion nucleophile.[58] These two zinc ions, as described by *Jozic et al.*,[55] were considered to play two different roles for hydrolyzing substrates: for stabilization of the substrate-enzyme tetrahedral intermediate as well as for activation of the catalytic water molecule. Moreover, the superimposition of the metal binding residues of PepD, PepV and CPG_2 were almost

indistinguishable except for Asp119 (Asp141) which was considered as the bridging residue held both two zinc ions in PepV (CPG_2). The orientation of Asp119 in PepD seems with less association for two zincs. However, mutants with losing activity provide some evidences for Asp119 involving in the catalytic reaction undoubtedly. Thus, we assumed that the active site pocket of PepD and PepV were similar and the hydrolytic mechanism might also be closely related but with slight difference.

Enzymes with the known crystal structures in M20 family such as PepV was identified as monomer whereas CPG_2 as homodimer in their native state. The native form of *V. alginolyticus* PepD was analyzed on the Native-PACE as well as western blotting analysis. Based on the Native-PAGE and the film, we assumed that both wild-type and mutant PepD existed in several forms while monomer form was formed in dominant. However, the result of analytical sedimentation velocity ultracentrifugation indicated that there were only homodimer in the native state of PepD .It is possible that none of the covalent interaction between PepD proteins was formed and non-covalent interaction was apparently weak. The dimerized PepD might be separated by electricity through electrophoresis analysis.

In conclusion, *V. alginolyticus* PepD was considered as a member of aminoacylhistidine dipeptidase which could hydrolyze Xaa-His dipeptides including an unusual dipeptide carnosine (β-Ala-L-His) with low catalytic efficiency. The further investigation on substrate specificity indicated that *V. alginolyticus* PepD was considered to be a Xaa-His dipeptidase that hydrolyze various His-containing dipeptides except the dipeptide with the negative charge in its N-terminal part. *V. alginolyticus* PepD is similar to the CN2 that could not hydrolyze the brain-specific dipeptidases such as GABA-His, but different from the PepV in losing the degradation ability toward unusual tripeptides. In native state, PepD existed in several forms but preferred to form homodimer. Mutagenesis study and

homology modeling structure on PepD revealed that the putative active site pocket of PepD might be similar to PepV, even the hydrolytic mechanism was closely related but with slight different. As a member of peptidase family M20, the most direct evidence on the metal content of PepD is determined through the progressive crystallization study for characterizing the mono- or di-zinc catalytic center. Either the actual active site pocket and hydrolytic mechanism will also be characterized via the crystallography.

Chapter 5 Future work

Based on the results in this study, two putative active site residues which were apparently involved in the catalysis of PepD were first identified. The saturated mutagenesis on other putative metal binding and catalytic sites will be continuous analyzed to clarify their roles in the peptidase activity of PepD. Moreover, several residues outside of the catalytic domain of enzymes in M20 family were considered to be involved in the substrate binding and catalysis in recent report. As described on section 1.9, the respective His269 from the lid domain of *L. delbrueckii* PepV was associated with Zn 1 for forming an oxyanion binding hole bound to the carbonyl oxygen of Glu 153 and led to a tetrahedral intermediate. This residue functioned for the stabilization of the transition state and its corresponding results to His229, His223, and His206 in the small domains of the dimeric homologs CPG2, PepT, and hAcy1 in M20 family were also be examined. The mutagenesis study on H206 of hAcyl in 2003[26] indicated that the conserved histidine in the dimerization domain of dimeric Acy1/M20 family enzymes contributes in *trans* to the active site. Therefore, several polar or aromatic residues outside of the putative active site of PepD should also be futher investigated by site-directed mutagenesis in the future.

PepD was identified as a member of metallopeptidases which required metal ion for its catalytic activity. In these peptidases, the metal ion is usually zinc but sometimes cobalt, manganese, nickel or copper. However, recent studies showed that different metal ion with various concentration could inhibit or increase the enzyme activity.[42, 64] The functional roles for the different metal centers as well as the activation mechanism due to lose metal ions are still unclear. Consequently, the metal selectivity and inhibition/activation mechanism will be valuable investigated in the future.

As the biological function of bacterial *pepD* is less understanding, the gene knock-out study on *V. alginolyticus pepD* followed by a series of biochemical or morphology analysis will provide more informations about its role in prokaryotes. At the same time, since PepD affects the bacterial biofilm formation, biofilm assay should also be performed and compared with both *V. alginolyticus* wild-type and *pepD* knockout strain.

With absence of the structure in neither peptidase family M20 nor similar peptidase, crystallization on the *V. alginolyticus* PepD was needed. Furthermore, the crystal structure of the wild-type and mutant proteins combined with the mutagenesis analysis data could provide an insight into the catalytic mechanism of bacterial aminoacylhistidine dipeptidase. Up to date, we have obtained the crystal of wild-type PepD with undesirable resolution. Therefore, the proceeding effort is still needed to modify the crystallization condition in order to improve the quality of crystal for further structure determination.

Chapter 6 Reference

1. Goarant, C.; Merien, F.; Berthe, F.; Mermoud, I.; Perolat, P., Arbitrarily primed PCR to type Vibrio spp. pathogenic for shrimp. *Appl Environ Microbiol* **1999,** 65, (3), 1145-51.

2. Miyamoto, Y., Nakamura, K., and Takizawa, K., Proposals of a new genus "Oceanomonas" and of the amended species names. *Jpn. J. Microbiol.* **1961,** 5, ( ), 477-86

3. Sakazaki, R., Proposal of Vibrio alginolyticus for the biotype 2 of Vibrio parahaemolyticus. *Jpn J Med Sci Biol* **1968,** 21, (5), 359-62.

4. Schmidt, U.; Chmel, H.; Cobbs, C., Vibrio alginolyticus infections in humans. *J Clin Microbiol* **1979,** 10, (5), 666-8.

5. Molitoris, E.; Joseph, S. W.; Krichevsky, M. I.; Sindhuhardja, W.; Colwell, R. R., Characterization and distribution of Vibrio alginolyticus and Vibrio parahaemolyticus isolated in Indonesia. *Appl Environ Microbiol* **1985,** 50, (6), 1388-94.

6. Rubin, S. J.; Tilton, R. C., Isolation of Vibrio alginolyticus from wound infections. *J Clin Microbiol* **1975,** 2, (6), 556-8.

7. Baross, J.; Liston, J., Occurrence of Vibrio parahaemolyticus and related hemolytic vibrios in marine environments of Washington State. *Appl Microbiol* **1970,** 20, (2), 179-86.

8. Paperna, I., Reproduction cycle and tolerance to temperature and salinity of Amyloodinium ocellatum (Brown, 1931) (Dinoflagellida). *Ann Parasitol Hum Comp* **1984,** 59, (1), 7-30.

9. Zen-Yoji, H.; Le Clair, R. A.; Ota, K.; Montague, T. S., Comparison of Vibrio parahaemolyticus cultures isolated in the United States with those isolated in Japan. *J Infect Dis* **1973,** 127, (3), 237-41.

10. Levine, W. C.; Griffin, P. M., Vibrio infections on the Gulf Coast: results of first year of regional surveillance. Gulf Coast Vibrio Working Group. *J Infect Dis* **1993,** 167, (2), 479-83.

11. Reina Prieto, J.; Hervas Palazon, J., [Otitis media due to Vibrio alginolyticus: the risks of the Mediterranean Sea]. *An Esp Pediatr* **1993,** 39, (4), 361-3.

12. Gahrn-Hansen, B.; Hornstrup, M. K., [Extraintestinal infections caused by Vibrio parahaemolyticus and Vibrio alginolyticus at the county of Funen 1987-1992]. *Ugeskr Laeger* **1994,** 156, (37), 5279-82.

13. Rippey, S. R., Infectious diseases associated with molluscan shellfish consumption. *Clin Microbiol Rev* **1994,** 7, (4), 419-25.

14. Blake, P. A.; Weaver, R. E.; Hollis, D. G., Diseases of humans (other than cholera) caused by vibrios. *Annu Rev Microbiol* **1980,** 34, ( ), 341-67.

15. Lipp, E. K.; Huq, A.; Colwell, R. R., Effects of global climate on infectious disease: the cholera model. *Clin Microbiol Rev* **2002,** 15, (4), 757-70.

16. Caccemese SM, R. D., Chronic diarrhea associated with Vibrio alginolyticus in an immunocompromised patient. *Clin Infect Dis.* **1999,** 29, ( ), 946-47.

17. Lessner, A. M.; Webb, R. M.; Rabin, B., Vibrio alginolyticus conjunctivitis. First reported case. *Arch Ophthalmol* **1985,** 103, (2), 229-30.

18. Lee, K. K., Pathogenesis studies on Vibrio alginolyticus in the grouper, Epinephelus malabaricus, Bloch et Schneider. *Microb Pathog* **1995,** 19, (1), 39-48.

19. Rawlings, N. D.; Barrett, A. J., Evolutionary families of metallopeptidases. *Methods Enzymol* **1995,** 248, ( ), 183-228.

20. Rawlings, N. D.; Morton, F. R.; Barrett, A. J., MEROPS: the peptidase database. *Nucleic Acids Res* **2006,** 34, (Database issue), D270-2.

21. Rawlings, N. D.; Barrett, A. J., Evolutionary families of peptidases. *Biochem J* **1993,** 290 (Pt 1), ( ), 205-18.

22. Wilcox, D. E., Binuclear Metallohydrolases. *Chem Rev* **1996,** 96, (7), 2435-2458.

23. Dismukes, G. C., Manganese Enzymes with Binuclear Active Sites. *Chem Rev* **1996,** 96, (7), 2909-2926.

24. Richard C Holz, Krzysztof P Bzymek and Sabina I Swierczek Co-catalytic metallopeptidases as pharmaceutical targets *Current Opinion in Chemical Biology* **2003,** 7,

(2), 197-206.

25. Wouters, M. A.; Husain, A., Changes in zinc ligation promote remodeling of the active site in the zinc hydrolase superfamily. *J Mol Biol* **2001,** 314, (5), 1191-207.

26. Lindner, H. A.; Lunin, V. V.; Alary, A.; Hecker, R.; Cygler, M.; Menard, R., Essential roles of zinc ligation and enzyme dimerization for catalysis in the aminoacylase-1/M20 family. *J Biol Chem* **2003,** 278, (45), 44496-504.

27. Friedlos, F.; Davies, L.; Scanlon, I.; Ogilvie, L. M.; Martin, J.; Stribbling, S. M.; Spooner, R. A.; Niculescu-Duvaz, I.; Marais, R.; Springer, C. J., Three new prodrugs for suicide gene therapy using carboxypeptidase G2 elicit bystander efficacy in two xenograft models. *Cancer Res* **2002,** 62, (6), 1724-9.

28. Brombacher, E.; Dorel, C.; Zehnder, A. J.; Landini, P., The curli biosynthesis regulator CsgD co-ordinates the expression of both positive and negative determinants for biofilm formation in Escherichia coli. *Microbiology* **2003,** 149, (Pt 10), 2847-57.

29. Klein, J.; Henrich, B.; Plapp, R., Cloning and expression of the pepD gene of Escherichia coli. *J Gen Microbiol* **1986,** 132, (8), 2337-43.

30. Schroeder, U.; Henrich, B.; Fink, J.; Plapp, R., Peptidase D of Escherichia coli K-12, a metallopeptidase of low substrate specificity. *FEMS Microbiol Lett* **1994,** 123, (1-2), 153-9.

31. van der Drift, C.; Ketelaars, H. C., Carnosinase: its presence in Pseudomonas aeruginosa. *Antonie Van Leeuwenhoek* **1974,** 40, (3), 377-84.

32. Bersani, M.; Crespi, F.; Giudici, V.; Bianchi, G., [Antral stenosis caused by gastric hemangioma]. *Minerva Chir* **1980,** 35, (17), 1283-6.

33. Miller, C. G.; Schwartz, G., Peptidase-deficient mutants of Escherichia coli. *J Bacteriol* **1978,** 135, (2), 603-11.

34. Kirsh, M.; Dembinski, D. R.; Hartman, P. E.; Miller, C. G., Salmonella typhimurium peptidase active on carnosine. *J Bacteriol* **1978,** 134, (2), 361-74.

35. Jackson, M. C.; Lenney, J. F., The distribution of carnosine and related dipeptides in rat

and human tissues. *Inflamm Res* **1996,** 45, (3), 132-5.

36. Boldyrev, A. A., Problems and perspectives in studying the biological role of carnosine. *Biochemistry (Mosc)* **2000,** 65, (7), 751-6.

37. Vaughan-Jones, R. D.; Spitzer, K. W.; Swietach, P., Spatial aspects of intracellular pH regulation in heart muscle. *Prog Biophys Mol Biol* **2006,** 90, (1-3), 207-24.

38. Decker, E. A.; Livisay, S. A.; Zhou, S., A re-evaluation of the antioxidant activity of purified carnosine. *Biochemistry (Mosc)* **2000,** 65, (7), 766-70.

39. Seidler, N. W., Carnosine prevents the glycation-induced changes in electrophoretic mobility of aspartate aminotransferase. *J Biochem Mol Toxicol* **2000,** 14, (4), 215-20.

40. Guiotto, A.; Calderan, A.; Ruzza, P.; Borin, G., Carnosine and carnosine-related antioxidants: a review. *Curr Med Chem* **2005,** 12, (20), 2293-315.

41. Petroff, O. A.; Hyder, F.; Rothman, D. L.; Mattson, R. H., Homocarnosine and seizure control in juvenile myoclonic epilepsy and complex partial seizures. *Neurology* **2001,** 56, (6), 709-15.

42. Teufel, M.; Saudek, V.; Ledig, J. P.; Bernhardt, A.; Boularand, S.; Carreau, A.; Cairns, N. J.; Carter, C.; Cowley, D. J.; Duverger, D.; Ganzhorn, A. J.; Guenet, C.; Heintzelmann, B.; Laucher, V.; Sauvage, C.; Smirnova, T., Sequence identification and characterization of human carnosinase and a closely related non-specific dipeptidase. *J Biol Chem* **2003,** 278, (8), 6521-31.

43. Lenney, J. F.; George, R. P.; Weiss, A. M.; Kucera, C. M.; Chan, P. W.; Rinzler, G. S., Human serum carnosinase: characterization, distinction from cellular carnosinase, and activation by cadmium. *Clin Chim Acta* **1982,** 123, (3), 221-31.

44. Wassif, W. S.; Sherwood, R. A.; Amir, A.; Idowu, B.; Summers, B.; Leigh, N.; Peters, T. J., Serum carnosinase activities in central nervous system disorders. *Clin Chim Acta* **1994,** 225, (1), 57-64.

45. Butterworth, R. J.; Wassif, W. S.; Sherwood, R. A.; Gerges, A.; Poyser, K. H.;

Garthwaite, J.; Peters, T. J.; Bath, P. M., Serum neuron-specific enolase, carnosinase, and their ratio in acute stroke. An enzymatic test for predicting outcome? *Stroke* **1996,** 27, (11), 2064-8.

46. Perry, T. L.; Hansen, S.; Tischler, B.; Bunting, R.; Berry, K., Carnosinemia. A new metabolic disorder associated with neurologic disease and mental defect. *N Engl J Med* **1967,** 277, (23), 1219-27.

47. Murphey, W. H.; Lindmark, D. G.; Patchen, L. I.; Housler, M. E.; Harrod, E. K.; Mosovich, L., Serum carnosinase deficiency concomitant with mental retardation. *Pediatr Res* **1973,** 7, (7), 601-6.

48. Vistoli, G.; Pedretti, A.; Cattaneo, M.; Aldini, G.; Testa, B., Homology modeling of human serum carnosinase, a potential medicinal target, and MD simulations of its allosteric activation by citrate. *J Med Chem* **2006,** 49, (11), 3269-77.

49. Hanson, H. T., and Smith, E. L., Carnosinase: an enzyme of swine kidney. *J. Biol. Chem.* **1949,** 179, ( ), 789-801.

50. Komeda, H.; Asano, Y., A DmpA-homologous protein from Pseudomonas sp. is a dipeptidase specific for beta-alanyl dipeptides. *Febs J* **2005,** 272, (12), 3075-84.

51. Walker, N. D.; McEwan, N. R.; Wallace, R. J., A pepD-like peptidase from the ruminal bacterium, Prevotella albensis. *FEMS Microbiol Lett* **2005,** 243, (2), 399-404.

52. Hellendoorn, M. A.; Franke-Fayard, B. M.; Mierau, I.; Venema, G.; Kok, J., Cloning and analysis of the pepV dipeptidase gene of Lactococcus lactis MG1363. *J Bacteriol* **1997,** 179, (11), 3410-5.

53. Vongerichten, K. F.; Klein, J. R.; Matern, H.; Plapp, R., Cloning and nucleotide sequence analysis of pepV, a carnosinase gene from Lactobacillus delbrueckii subsp. lactis DSM 7290, and partial characterization of the enzyme. *Microbiology* **1994,** 140 (Pt 10), ( ), 2591-600.

54. Biagini, A.; Puigserver, A., Sequence analysis of the aminoacylase-1 family. A new

proposed signature for metalloexopeptidases. *Comp Biochem Physiol B Biochem Mol Biol* **2001,** 128, (3), 469-81.

55. Jozic, D.; Bourenkow, G.; Bartunik, H.; Scholze, H.; Dive, V.; Henrich, B.; Huber, R.; Bode, W.; Maskos, K., Crystal structure of the dinuclear zinc aminopeptidase PepV from Lactobacillus delbrueckii unravels its preference for dipeptides. *Structure* **2002,** 10, (8), 1097-106.

56. Chevrier, B.; Schalk, C.; D'Orchymont, H.; Rondeau, J. M.; Moras, D.; Tarnus, C., Crystal structure of Aeromonas proteolytica aminopeptidase: a prototypical member of the co-catalytic zinc enzyme family. *Structure* **1994,** 2, (4), 283-91.

57. Greenblatt, H. M.; Almog, O.; Maras, B.; Spungin-Bialik, A.; Barra, D.; Blumberg, S.; Shoham, G., Streptomyces griseus aminopeptidase: X-ray crystallographic structure at 1.75 A resolution. *J Mol Biol* **1997,** 265, (5), 620-36.

58. Rowsell, S.; Pauptit, R. A.; Tucker, A. D.; Melton, R. G.; Blow, D. M.; Brick, P., Crystal structure of carboxypeptidase G2, a bacterial enzyme with applications in cancer therapy. *Structure* **1997,** 5, (3), 337-47.

59. Csampai, A.; Kutlan, D.; Toth, F.; Molnar-Perl, I., o-Phthaldialdehyde derivatization of histidine: stoichiometry, stability and reaction mechanism. *J Chromatogr A* **2004,** 1031, (1-2), 67-78.

60. Yiallouros, I.; Kappelhoff, R.; Schilling, O.; Wegmann, F.; Helms, M. W.; Auge, A.; Brachtendorf, G.; Berkhoff, E. G.; Beermann, B.; Hinz, H. J.; Konig, S.; Peter-Katalinic, J.; Stocker, W., Activation mechanism of pro-astacin: role of the pro-peptide, tryptic and autoproteolytic cleavage and importance of precise amino-terminal processing. *J Mol Biol* **2002,** 324, (2), 237-46.

61. Hansenb, J. L. C. a. J. C., Analytical Ultracentrifugation as a Contemporary Biomolecular Research Tool *Journal of Biomolecular Techniques* **1999,** 10, (4), 163-176.

62. Stafford, W. F., Sedimentation velocity spins a new weave for an old fabric. *Curr Opin*

Biotechnol **1997,** 8, (1), 14-24.

63. Kelly, S. M.; Jess, T. J.; Price, N. C., How to study proteins by circular dichroism. *Biochim Biophys Acta* **2005,** 1751, (2), 119-39.

64. Lai, W. L.; Chou, L. Y.; Ting, C. Y.; Kirby, R.; Tsai, Y. C.; Wang, A. H.; Liaw, S. H., The functional role of the binuclear metal center in D-aminoacylase: one-metal activation and second-metal attenuation. *J Biol Chem* **2004,** 279, (14), 13962-7.

Appendix 1

Primers used in this thesis

Sequencing and Expression		
F1 (sense)	5’-GTGTCTGAGTTCCATTC-3’	(1-17)[a]
F2 (sense)	5’-TGGGCGACAGAGCAAGG-3’	(127-143)
F3 (sense)	5’-TCTGGCGCTTACCCAGG-3’	(1189-1205)
R1 (antisense)	3’-AAGGACTTTTCCGCATT-5’	(1457-1473)
R2 (antisense)	3’-CGTAACTTGCGAACAGG-5’	(979-995)
R3 (antisense)	3’-GTGACTAGTGCTGAAGT-5’	(270-286)
N1 (sense)	5’-CGCGGATCCCATATGGTGTCTGAGTTCCATTC-3’	(*Nde*I)[b]

Mutagenesis		
D119X-1	5’-CGCTCGGGGCANNNAACGGCATCGGCATGGC-3’	(*Ava*I)
D119X-2	5’-GCCATGCCGATGCCGTTNNNTGCCCCGAGCG-3’	(*Ava*I)
E149X-1	5’-CTGACAATTGATNNNGAAGCAGGCATGACAGG-3’	(*Mfe*I)
E149X-2	5’-CCTGTCATGCCTGCTTCNNNATCAATTGTCAG-3’	(*Mfe*I)

Appendix 2

The restriction enzyme used in expresson vectors check and the expected size of excised fragment.

Plasmid	R.E.[a] used	Excised frangment
pET-pepD-WT	*Ava*I	-[b]
pET-pepD-D119X	*Ava*I	1.2 kbp.
pET-pepD-WT	*Pvu*I	-[b]
pET-pepD-E149A	*Mfe*I/*Not*I	1.2 kbp.

[a] R.E.= restriction enzymes.
[b] No expected DNA fragment was excised.

Appendix 3

Experimental Materials

◆ Bacterial strains, plasmids, animal, and cell

Escherichia coli BL21(DE3)pLysS (Novagen)

Escherichia coli XL1-Blue (Novagen)

Vibrio alginolyticus ATCC 17749 (FIRDI, Taiwan)

pCR®2.1-TOPO (Invitrogen)

pET-28a(+) (Novagen)

Female BALB/c mice (National Science Council, Taiwan)

Mouse myeloma cell line FO (FIRDI, Taiwan)

◆ Chemicals and Reagents

Acetic acid (Merck)

Acrylamide (GE Healthcare)

Agarose (USB)

α-Ala-L-His (Sigma)

APS (GE Healthcare)

β-Asp-L-His (Sigma)

Bacto™ Agar (DIFCO)

Bestatin (MP Biomedicals)

Bovine Calf Serum (HyClone)

Bromophenol blue (USB)

L-carnosine (ICN Biomedicals, Inc.)

Citric acid (Sigma)

Coomassie® Brilliant blue R 250 (Merck)

Dimethylformamide (Merck)

Dimethyl sulfoxide (MP Biomedicals)

Dodecyl sulfate sodium salt (Merck)

Dulbecco's Modified Eagle Medium (Gibco)

dNTP Set, 100 mM Solutions (GE Healthcare)

Ethylenediamine-tetraacetic acid (Merck)

GABA-His (Sigma)

L-glutamine solution 100X, 200mM (biowest)

Glycerol (Merck)

Glycine (Merck)

Gly-Gly-His (Sigma)

Gly-His (Sigma)

Gly-His-Gly (Sigma)

HAT Media Supplement (50X) Hybri-Max® (Sigma)

L-histidine (Sigma)

His-His (Bachem)

His-Ile (Bachem)

His-Val (Bachem)

L-homocarnosine (Sigma)

HT Supplement (100X), liquid (GIBCO)

Hydrogen chloride (Merck)

Ile-His (Bachem)

Imidazole (USB)

IPTG (GeneMark, Taiwan)

Kanamycin sulfate (USB)

LB Broth, Miller (DIFCO)

Leu-His (Bachem)

2-mercaptoethanol (Merck)

Methanol (Merck)

N,*N*'-methylene-bis-acrylamide (Sigma)

Ni-NTA His-Band® Resin (Novagen)

Penicillin-Streptomycin Solution 100X (biowest)

o-phthaldialdehyde (Merck)

Potassium chloride (Merck)

Potassium diphosphate (Merck)

Potassium phosphate (Merck)

Primers (Bio Basic Inc., Taiwan)

Restriction enzymes (New England Biolabs)

Ser-His (Bachem)

Sodium azide (Merck)

Sodium chloride (AMRESCO)

Sodium hydroxide (Merck)

SYBR® Green I (Roche)

T4 DNA ligase (Promega)

TEMED (GE Healthcare)

Trichloroacetic acid (Merck)

Tris base (USB)

Tryptic soy broth (ALPHA BIOSCIENCES)

Tyr-His (Bachem)

Val-His (Bachem)

X-gal (GeneMark, Taiwan)

◆ Kits

BCA Protein Assay Reagent and Albumin Standard (PIERCE)

BigDye® Terminator v3.1 Cycle Sequencing Kit (Applied Biosystems)

GFX™ PCR DNA and Gel Band Purification Kit (GE Healthcare)

HMW Native Marker Kit (GE Healthcare)

LMW-SDS Marker Kit (GE Healthcare)

QIAamp DNA Mini Kit (Qiagen)

TOPO TA Cloning® Kit (Invitrogen)

Plasmid Miniprep Purification Kit (GeneMark)

r*Tth* DNA polymerase, XL & XL Buffer II Pack (Applied Biosystems)

◆ Equipments

25 cm^2 flask (NUNC)

ABI PRISM® 3100 Genetic Analyzer (Applied Biosystems)

Allegra™ 21R Centrifuge (Beckman Coulter)

Avanti® J-E Centrifuge (Beckman Coulter)

Blood Collecting Tubes (Chase Scientific Glass, Inc.)

Centrifuges 5415R (eppendorf)

Colling Circulator Bath Model B401L (Firstek Scientific)

Compact Tabletop Centrifuge 2100 (KUBOTA)

Dri-Bath Type 17600 (Thermolyne)

Durabath™ Water Bath (Baxter)

Econo-Pac Columns (BIO-RAD)

Electrophoresis Power Supply EPS 301 (GE Healthcare)

EPSON® GT-7000 Scanner (EPSON)

F96 MicroWell™ plate (black) (NUNC)

F96 MicroWell™ plate (clear) (NUNC)

Fisher Vortex Genie 2™ (Fisher Scientific)

Fluoroskan Ascent FL Microplate Reader (Thermo)

GeneAmp® PCR System 9700 Thermal Cycler (Applied Biosystems)

Hoefer® HE 33 Mini Horizontal Submarine Unit (GE Healthcare)

Hoefer® Mighty Small dual gel caster (GE Healthcare)

Kodak Electrophoresis Documentation and Analysis System 120 (Kodak)

Mighty Small II for 8×7 cm gels electrophoresis instruments (GE Healthcare)

Millex®-GS 0.22 μm Filter Unit (Millipore)

Millex®-HA 0.45 μm Filter Unit (Millipore)

Multiskan Ascent Microplate Reader (Thermo)

Orbital shaking incubator Model S300R (Firstek Scientific)

Rocking Shacker Model RS-101 (Firstek Scientific)

Steritop™ 0.22 μm Filter Unit (Millipore)

Ultrasonic Processor VCX 500/750 (Sonics)

US AutoFlow™ NU 4000 Series CO_2 Water-Jacketed Incubator (NuAire)

UV-Visible Spectrophotometer Ultrospec 3100 pro (GE Healthcare)

◆ Solutions

Blocking buffer

5% non-fat milk in distilled water (dH_2O).

Destain buffer I

Mix 400 mL methanol, 100 mL acetic acid and dH_2O to 1 L. Store at room temperature (RT).

Destain buffer II

Mix 50 mL methanol, 120 mL acetic acid and distilled water (dH_2O) to 1 L. Store at RT.

6X DNA loading dye

0.25% bromophenol blue and 30% glycerol in double distilled water (ddH_2O). Store at -20℃.

IPTG stock solution

Dissolve 4.0863 g IPTG in 10 mL ddH_2O. Filter through 0.22 μm pore size filter and store at -20℃.

Kanamycin stock solution

Dissolve 250 mg kanamycin sulfate in 10 mL ddH_2O. Filter through 0.22 μm pore size filter and store at -20℃.

LB medium

25 g LB Broth was dissolved in 1 L dH_2O and sterilized.

LB plate

25 g LB Broth and 20 g Bacto^{TM} Agar was dissolved in 1 L dH_2O and sterilized. The sterile LB agar was poured and dispersed in petri dishes before it coagulates.

10X Native-PAGE running buffer

Dissolve 144 g glycine and 30 g Tris base in 1 L dH_2O and store at 4℃. Dilute to 1X with dH_2O before use.

5X Native-PAGE sample buffer

8 mg bromophenol blue, 1.7 mL 0.5 M Tris-HCl, pH 6.8, 5 mL glycerol, and 4 mL dH_2O were mixed and stored at -20℃.

OPA reagent (for enzyme kinetics)

Dissolve 50 mg OPA in 5 mL methanol first and then mix with 20 mL borate buffer. The borate buffer was mixed by 0.2 M boric acid (dissolved in 0.2 M potassium chloride solution) and 0.2 M sodium hydroxide solution (50: 50, v/v). The OPA reagent was stored in darkness at 4℃ for no longer than 9 days and prepared at least 90 min earlier before use.

10X PBS buffer

Dissolve 13.7 g Na_2HPO_4, 3.5 g NaH_2PO_4, and 87.7 g NaCl in 1 L dH_2O and store at RT. Dilute to 1X with dH_2O and sterilize before use.

10X SDS-PAGE running buffer

Dissolve 144 g glycine, 30 g Tris base, and 10 g SDS in 1 L dH_2O and store at 4℃. Dilute to 1X with dH_2O before use.

5X SDS-PAGE sample buffer

8 mg bromophenol blue, 1.7 mL 0.5 M Tris-HCl, pH 6.8, 0.5 mL 20% (w/v) SDS, 2 mL 2-mercaptoethanol, 5 mL glycerol, and 4 mL dH_2O were mixed and stored at -20℃.

Stain buffer

Dissolve 1 g Coomassie Brilliant blue R-250 in 500 mL methanol first. Then add 100 mL acetic acid and dH_2O to 1 L final volume. Filter through reused 0.22 μm pore size filter and store at RT.

50X TAE buffer

Dissolve Tris base 242 g, acetic acid 57.1 mL, and 0.5 M EDTA in 1 L dH_2O and adjust to pH 8.5. Dilute to 1X with dH_2O and adjust to pH 7.5-7.8 before use.

10X Western transfer buffer

Dissolve 144 g glycine, 30 g Tris base, and 10 g SDS in 1 L dH_2O and store at 4℃. Dilute to 1X with dH_2O before use.

X-gal stock solution

Dissolve 400 mg X-gal in 10 mL dimethylformamide (DMF) and store in the darkness at -20℃.